Peer review status: This is a non-peer-reviewed preprint submitted to EarthArXiv

Rapid increase of climate extremes across northern Amazonia

Authors

Jos Barlow[1], Nathália Carvalho[1], Cássio Alencar Nunes[1], Ana Paula Dutra Aguiar[2], Ane Alencar[3], Liana Anderson[2], Luiz E.O.C Aragao[2], Fabricio Baccaro[4], Mike Barrett[5], Erika Berenguer[6], Kristian Bodolai[7], Paulo Monteiro Brando[8], Thiago B A Couto[9], Tomas Ferreira Domingues[10], Fernando Elias[11], Ted R. Feldpausch[12], Igor José Malfetoni Ferreira[2], Joice N. Ferreira[11], Bernardo M. Flores[13], David Galbraith[14], Toby Alan Gardner[15], Emanuel Gloor[14], Marina Hirota[16], Val Kapos[17], David M. Lapola[18], Cecília Leal[1], Alexander Charles Lees[19], Bel Lyon[5], Marcia Macedo[20], Yadvinder Malhi[6], Beatriz Schwantes Marimon[21], Ben Hur Marimon Junior[21], Patrick Meir[22], Lina M Mercado[12], Oliver Metcalf[1], Leonardo De Sousa Miranda[1], Edward Mitchard[7], Douglas C. Morton[23], Jeanne L. Nel[24], Rafael Silva Oliveira[18], Oliver Phillips[14], Lucy Rowland[12], Juliana Schietti[25], Camila S.J. Silva[3], Celso H. L. Silva-Junior[3], Patrícia S. Silva[8], Juliana M. Silveira[1], Divino Vicente Silverio[26], Stephen Sitch[12], Paulo Amador Tavares[27], Cristina Telhado[17], Ima Vieira[28], Helga Correa Wiederhecker[29]

Institutions

1. Lancaster Environment Centre, Lancaster University, UK, 2. National Institute for Space Research – INPE, Brazil, 3. Amazon Environmental Research Institute (IPAM), Brazil. 4. Universidade Federal do Amazonas, Brazil. 5. WWF-UK. 6. Environmental Change Institute, School of Geography and the Environment, University of Oxford, UK, 7. Space Intelligence, UK. 8. Yale School of the Environment, Yale University, New Haven, CT, USA, 9. University of East Anglia, UK, 10. Departmento de Biologia - FFCLRP-USP, Brazil. 11. Embrapa Amazonia Oriental, Belem, Brazil. 12. Faculty of Environment, Science and Economy, University of Exeter, Exeter, UK. 13. Instituto Juruá, Manaus, Brazil. 14. University of Leeds, UK. 15. Stockholm Environment Institute, Sweden. 16. Federal University of Santa Catarina, Brazil. 17. WCMC-UNEP, UK. 18. Universidade Estadual de Campinas – UNICAMP, Brazil. 19. Manchester Metropolitan University, UK. 20. Columbia University, New York, USA. 21. State University of Mato Grosso UNEMAT, Brazil. 22. University of Edinburgh, UK. 23. NASA Goddard Space Flight Center, USA. 24. Wageningen University C Research, Netherlands. 25. Instituto Nacional de Pesquisas da Amazônia (INPA), Brazil. 26. Universidade Federal Rural da Amazônia, Brazil. 27. Universidade do Estado do Amapá, Brazil. 28. Museu Paraense Emilio Goeldi, Brazil. 29. WWF-Brazil

Abstract

Amazonia's exceptional biodiversity, cultural significance, and ecosystem services make it pivotal to global and regional sustainability. However, the region is increasingly threatened by climate extremes, which exacerbate the effects of land use change (Barlow et al., 2018) and bring about abrupt changes in social and ecological condition (Bennett et al., 2023; Berenguer et al., 2021; Campanharo et al., 2022; Lapola et al., 2023; Libonati et al., 2022; Lima et al., 2024; Machado-Silva et al., 2020; Tadano et al., 2024). Yet, while climate extremes are increasing in many parts of the world (Huntingford et al., 2024), we lack a high-resolution Amazon-wide assessment that compares if they differ from climate averages or identifies spatial hotspots where rates of change are highest. Here we address this by assessing Amazonia's changing climate at high spatial resolution within seasons and across the year, considering both central trends (50th percentile) and trends of extremes (5th and 95th percentiles). Our analysis includes a new measure of water deficit that accounts for the effects of temperature on evapotranspiration. High temperature extremes and temperature-linked measures of water deficit are both changing at a much faster rate than central trends, and their rates of change are greatest in the driest period. While the central trend of mean temperature change across Amazonia (0.21°C per decade, dec^{-1}) is comparable to the global average, the upper extreme of maximum temperatures in the driest period increased by 0.50°C dec^{-1}. These Amazon-wide trends also mask considerable spatial variation. Crucially, we identify a new region of high climate risk in central-north Amazonia, where over 700,000 square kilometres have experienced increases in extreme dry season temperatures of at least 0.77 °C dec^{-1} (i.e., ≥3.31 ºC over 43 years). Adaptation measures are urgently required to address the impacts of these rapid changes in climate extremes, including preventing the key stressors of deforestation, forest fires and other disturbances that amplify climate risks.

Main

The frequency and intensity of climate extremes have increased in many regions of the world (Huntingford et al., 2024) and are predicted to increase further under future climate change scenarios (Dosio et al., 2018). These extremes are responsible for some of the greatest climate-linked impacts on nature and people, driving increases in human morbidity and mortality (Ebi et al., 2020; IPCC et al., 2022), losses of forest species (Kotz et al., 2025) and ecosystem degradation (Maxwell et al., 2018). Climate extremes are also responsible for deleterious changes in some of the world's most important ecosystems. In Amazonia, recent exceptionally hot or dry periods have led to extensive and unprecedented forest fires (Alencar et al., 2015; Aragão et al., 2018; Berenguer et al., 2021), large-scale tree mortality (Bennett et al., 2023) and localised animal mortality (Guimaraes et al., 2025), and negative outcomes for human access to services (Lima et al., 2024) and health (Campanharo et al., 2022; Libonati et al., 2022; Machado-Silva et al., 2020). An increase in the incidence and severity of climate extremes could therefore help push Amazonia past critical thresholds, leading to much larger-scale deterioration of social and ecological conditions (Brando et al., 2025; Flores et al., 2024; Lapola et al., 2023).

Given the importance of climate extremes as drivers of change in Amazonia, it is crucial to understand the temporal and spatial distribution of change. Although the central trends of temperature change in Amazonia are tracking global averages (Gatti et al., 2021; Jiménez-Muñoz et al., 2013; Marengo et al., 2024), these are often poor predictors of the trends of climate extremes (Huntingford et al., 2024). This is particularly the case in South America, where the divergences between changes in mean and extreme temperatures are widespread, but variable (Huntingford et al., 2024). Inferences from global, pantropical or regional studies on climate extremes are currently insufficient. Many report only annual averages, which are known to mask ecologically important seasonal changes (Gloor et al., 2013). Others simplify the substantial spatial and temporal heterogeneity in dry season length and onset that exists across Amazonia (Carvalho et al., 2021a), Extended Data Figure S1) by defining dry season timing according to the drier period in the southern Amazon (Espinoza et al., 2024; Jiménez-Muñoz et al., 2013; Qin et al., 2025) or across large sub-regions (Franco et al., 2025; Gatti et al., 2021; Marengo et al., 2024). In addition, most focus on changes in either temperature, precipitation or water deficit, and therefore fall short of the integrated approach required to understand drivers of key ecological responses such as vegetation productivity and mortality (Tavares et al., 2023) and forest flammability (Ray et al., 2005). Finally, in the Amazon, climate change is overlain on high rates of deforestation (Silva-Junior et al., 2021) and degradation (Lapola et al., 2023), amplifying the impacts on forests and rivers (Barlow et al., 2018). New understanding of the spatial association between climate extremes and land-use change represents an important advance in helping to determine regions at risk.

Here, we provide a comprehensive assessment of the changing central (50^{th} percentile) and extreme trends (5^{th} and 95^{th} percentiles) of multiple climate variables across the 7 million km^2 region of Amazonia (see Methods), based on 11 km spatial resolution (57,900 grid cells) from 1981 to 2023 (43 years). We divide the year into 73 pentads to explore changes across hydrological years, following approaches used to identify changes in dry season timing across extensive subregions (Fu et al., 2013; Marengo et al., 2024). However, we extend this so that each grid square has its own hydrological periodicity, with annual or seasonal periods starting with the wettest pentad or month instead of calendar years or fixed months (Extended Data Figure S2). This allowed us to assess daily averages of minimum, mean and maximum temperature and Vapour Pressure Deficit (VPD) during the driest period as well as across the hydrological year. For rainfall, we evaluated driest and wettest period and the intensification of the water cycle through changes in rainfall amplitude. We also integrate changes in temperature with changes in rainfall or humidity, analysing variation in VPD and Maximum Cumulative Water Deficit (MCWD) that are well-established predictors of both plant physiology and fire activity (Aragão et al., 2007; Brando et al., 2014). MCWD was calculated in two ways: using a fixed 100 mm of evapotranspiration per month commonly used in the literature (MCWD100; Aragão et al., 2007; Silva-Junior et al., 2019) and by allowing evapotranspiration to increase with temperature ($MCWD_{Temp}$) following modelled estimates of temperature and atmospheric $C0_2$ responses (Malhi et al., 2009) that are broadly supported by recent observations (Laipelt et al., 2025). Finally, we identified the metrics and regions showing the greatest rate of change, and assessed whether these are associated with regions that were historically warmer or drier, or that have suffered the greatest amount of conversion from forest to agricultural land. We discuss these results considering their implications for climate adaptation, conservation and sustainability in Amazonia.

Climate change across Amazonia

On average, the rate of change of extreme temperatures from 1981 to 2023 was faster than the central trend (Figure 1, Extended Data Figure S3). For central trends, annual mean temperatures increased by a mean rate of 0.21 °C per decade (dec^{-1}) (Interquartile Range IQR: 0.15-0.27 ºC dec^{-1}) and 0.90 °C between 1981-2023, which is in line with the global average and previous estimates for Amazonia (Jiménez-Muñoz et al., 2013) (Figure 1a). However, the 95^{th} percentile of mean temperatures increased at a mean rate of at least 0.30 ºC dec^{-1} (IQR:0.24-0.37 ºC dec^{-1}) and 1.29 ºC over 43 years (Figure 1a). As expected, the rate of increase was greater in the driest period than across the whole hydrological year (Gatti et al., 2021), with maximum temperature at the 95th percentile increasing by 0.50 ºC dec^{-1} (IQR: 0.36-0.64 ºC dec^{-1}) (Figure 1a). This corresponds to an increase of 2.15 °C over 43 years, 2.38 times higher than the annual mean central trend (Figure 1a).

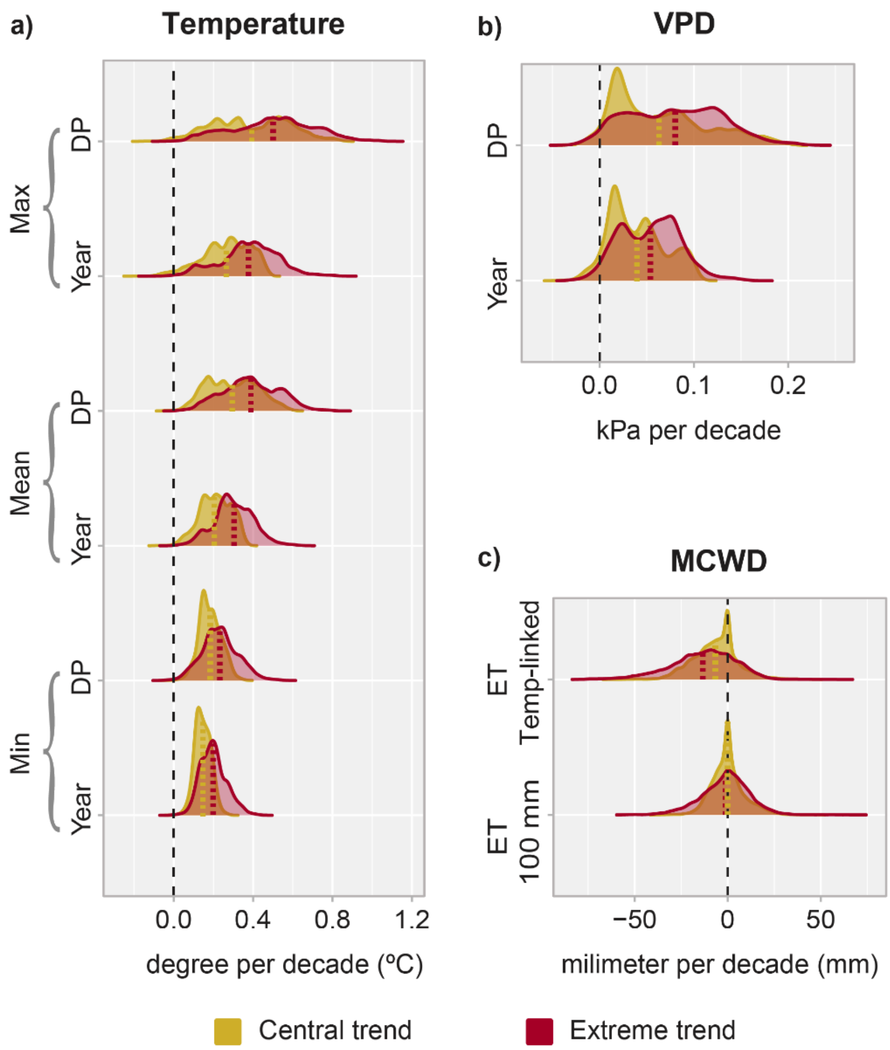

Figure 1. The magnitude of climate change across the Amazon region over 43 years (1981-2023). Decadal rates of change of a, temperature (ºC per decade) b, vapour-pressure deficit (VPD; kPa per decade) and c, maximum cumulative water deficit (MCWD; mm per decade). All panels show the rate of change for the central trend (50th percentile) and extreme (5th percentile for MCWD; 95th percentile for temperature and VPD), calculated on grid cell-wise with a spatial resolution of 11 km. Trends for minimum, mean and maximum temperature and mean VPD were calculated for the hydrological year (Year) and driest period (DP) considering pentad means (5-day period). MCWD was calculated considering two evapotranspiration (ET) thresholds, one fixed at 100 mm and the other linked to temperature. In all panels, coloured dashed lines represent the Amazon-wide mean rate of change per decade for each variable in each period for the central (yellow) and extreme (red) trends. Black dashed vertical lines correspond to zero. The panel for all variables is available in Extended Data Figure S3.

Temperature-linked measures of maximum cumulative water deficit ($MCWD_{Temp}$) and the vapour pressure deficit (VPD) also showed large changes over time, with higher values for extreme percentiles. For VPD, increases in the 95th percentiles were about one-third higher than for the central trend, for both annual and driest periods (Figure 1b). VPD also had the greatest rate of change during the driest period, increasing by 0.06 kPa dec^{-1} at the central trend (IQR: 0.02-0.09 kPa dec^{-1}) and 0.26 kPa over 43 years. This was even higher at the 95th percentile, increasing by 0.08 kPa dec^{-1} (IQR :0.04-0.12 kPa dec^{-1}; 0.34 kPa over 43 years) (Figure 1b). For MCWD, which is scaled towards the negative, the 5th percentile represents the drier extreme. The mean rate of change at the 5th percentile of $MCWD_{Temp}$ was -13.18 mm dec^{-1} (IQR: -23.58 to -0.93 mm dec^{-1}) and -56.67 mm over 43 years. This was twice that of the central trend of $MCWD_{Temp}$ of -6.60 mm dec^{-1} and -28.38 mm over 43 years (Figure 1c). The temperature-invariant measure of $MCWD_{100}$ showed no directional trend, with the 50th percentile changing by just 0.04 mm dec^{-1} (IQR: -5.27 to 4.01 mm dec^{-1}) and 0.17 mm over 43 years (Extended Data Figure S3b).

Precipitation increased across the central, 5th and 95th percentiles for both annual and wettest periods of the year, but the trends were close to zero when assessing only the driest period (Extended Data Figure S3d). For the central trend, annual precipitation increased by a mean rate of 31.47 mm dec^{-1} (IQR: -8.44 – 65.50) and 135.32 mm over 43 years; Extended Data Figure S3d). Precipitation amplitude showed a slight increase at all percentiles, with the greatest at the 95th percentile, where intensification of the water cycle – the difference between the wettest and driest periods – rose by a mean rate of 14.80 mm dec^{-1} (IQR: -20.79 - 52.72 mm dec^{-1}) or 63.64 mm over 43 years (Extended Data Figure S3e).

Spatial variation and hotspots of climate change

Amazonia-wide averages encompass considerable regional variation, with pronounced spatial divergence among the regions most affected by the highest rates of change at the 50th and extreme percentiles (Figure 2, Extended Data Figure S4-S8). For the central trend of change across the hydrological year, our results are broadly consistent with previous work and the southern Amazon stands out as the region most affected by increases in temperature and temperature-linked variables such as VPD (Figure 2, Extended Data Figure S4, S5) (Gatti et al., 2021; Marengo et al., 2022). However, at the 95th percentile, the greatest rates of change for temperature and VPD are concentrated in a central-northern region (Figure 2a-b) that has rarely been identified as being imperilled by climate change. Here, changes in average maximum temperature and mean VPD in the driest period were particularly alarming, with 10% of the biome surpassing rates of increase of 0.77 ºC dec^{-1} (>3.31 ºC over 43 years) and 0.14 kPa dec^{-1} (>0.60kPa over 43 years). The region was also a locus of change in $MCWD_{temp}$, with extreme years seeing rates of change of -36.45 mm dec^{-1} <-156.74 mm over 43 years) (Figure 2).

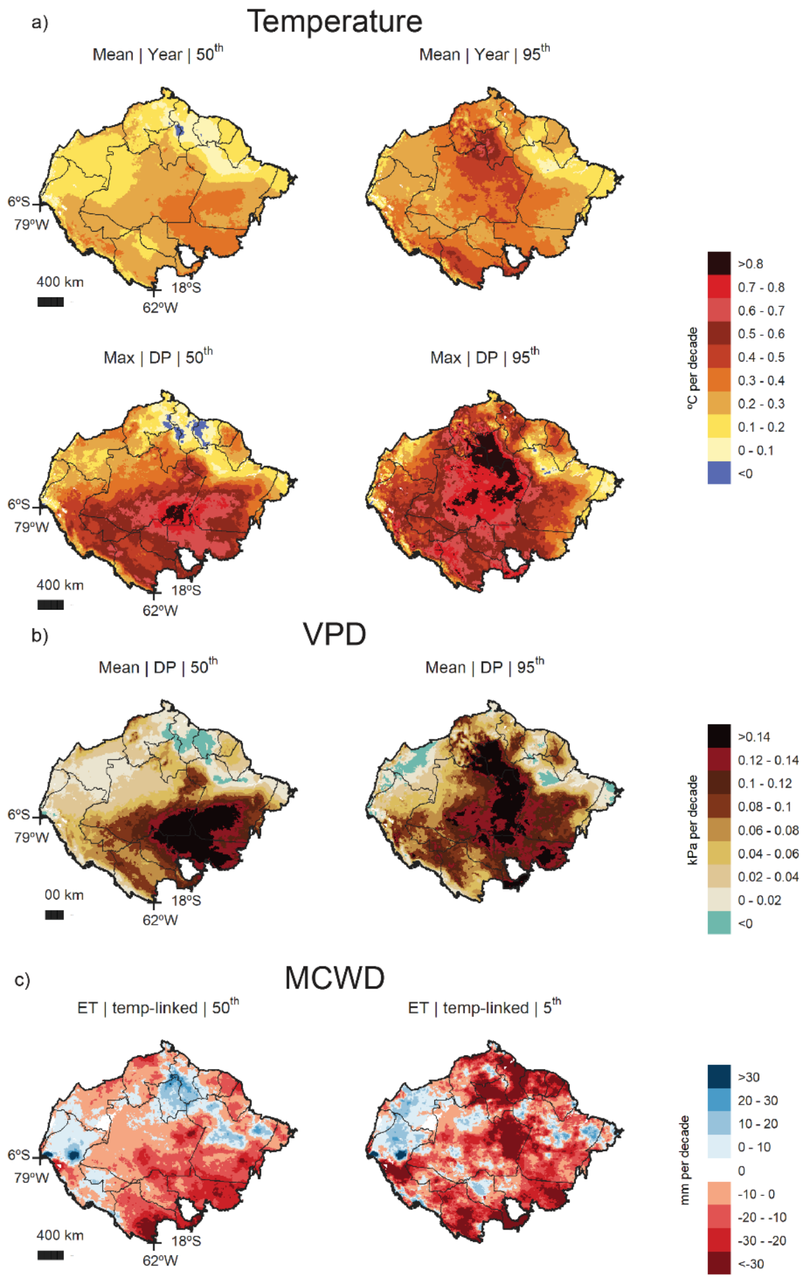

Figure 2. Spatial distribution of climate change across the Amazon over 43 years (1981-2023). Decadal rate of change were calculated grid cell-wise at 11 km spatial resolution for **a,** the mean and maximum temperature **b,** mean vapour-pressure deficit (VPD) and **c,** maximum cumulative water deficit (MCWD). The rates of change for temperature (ºC per decade) and VPD (kPa per decade) are shown, along with both the central (50^{th}) and upper extreme (95^{th} percentile) trends, for the hydrological year (Year) and the driest period (DP). For MCWD, the rate of change is shown for the central trend (50^{th} percentile) and the lower extreme (5^{th} percentile) considering a temperature-linked evapotranspiration threshold. Maps for all variables, percentiles and periods are available in Extended Data Figure S4-S8.

There was a strong spatial signal to the difference between central and extremes rates of climate change (Figure 3). In much of the southern and southern-eastern Amazon, central trends are growing at a similar rate to – or even slightly faster than – the 95^{th} percentile of temperature and VPD or 5^{th} percentile of $MCWD_{temp}$. In contrast, in the central-north region the rate of change of climate extremes (95th percentiles for temperature and VPD, 5th percentiles for $MCWD_{temp}$) diverged greatly from both the central trends and the opposite extremes (Figure 3a). Overlaying the top deciles of rates of change at the central and most extreme trends (95th percentile for mean temperature in the hydrological year, maximum temperature and VPD in the driest period of the hydrological year with the 5th percentile for $MCWD_{Temp}$) highlights critical regions where the fastest rates of change are co-occuring (Figure 4). For central trends, there was strong spatial agreement between temperature and VPD, while $MCWD_{Temp}$ was also prevalent on the southern borders of Amazonia. For the extreme trends, temperature-VPD overlaps were also extensive, but critical areas for $MCWD_{Temp}$ included additional regions at the periphery of Amazonia (Figure 4). These regions of greatest risk from rising central and extreme trends are predominantly located within Brazil and overlap with many important protected areas and indigenous lands (Extended Data Figure S9).

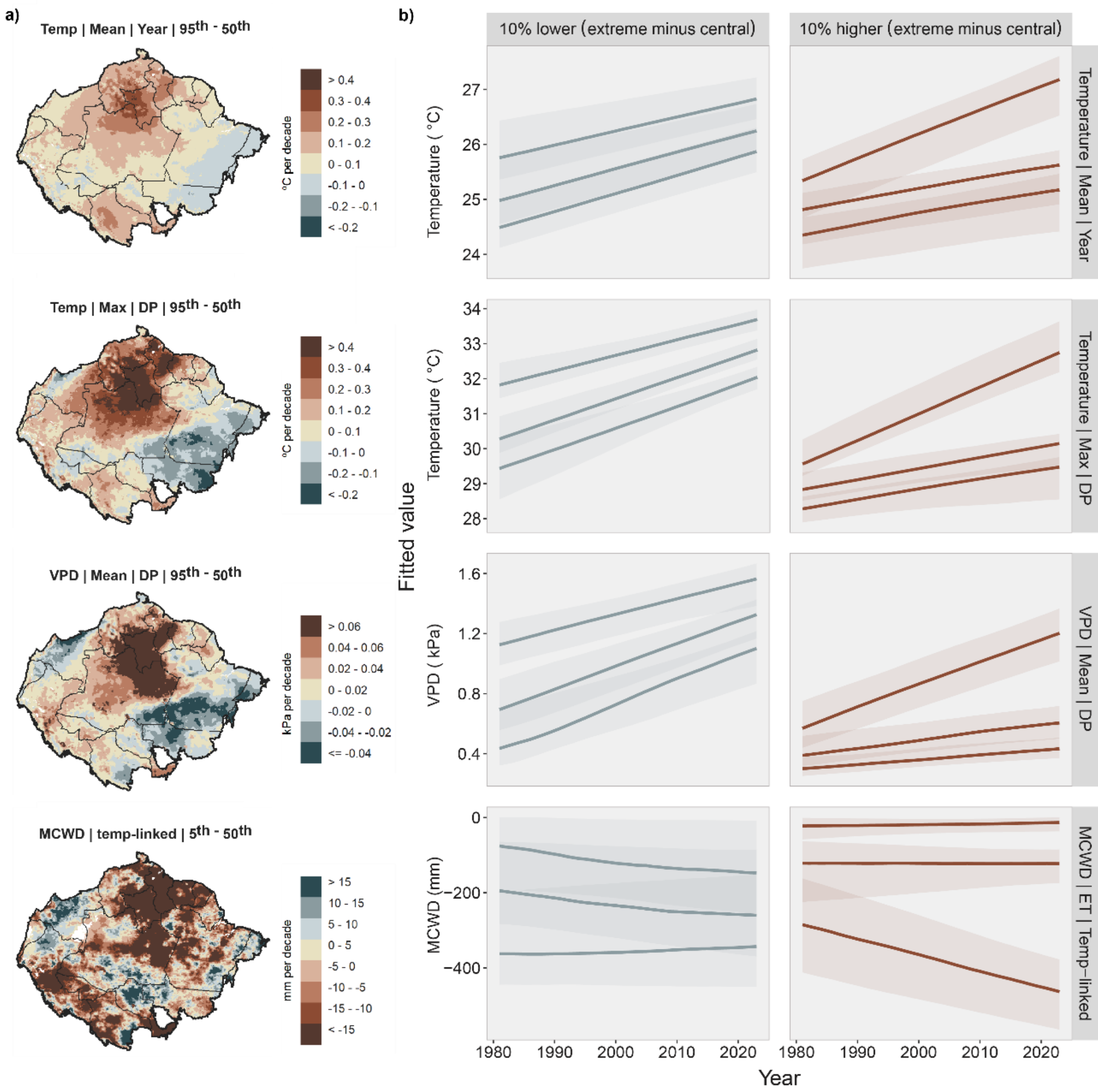

Figure 3. Spatial difference in the slope of change between extreme and central percentiles, highlighting trends of change in regions with the highest and lowest values differences. a, Difference between the rate of change in

extreme and central (50th percentile) trend was calculated per cell for mean temperature (hydrological year, 95th percentile), maximum temperature (driest period, 95th percentile), vapour-pressure deficit (VPD, driest period, 95th percentile) and maximum cumulative water deficit (MCWD, temperature-linked, 5th percentile). In all maps, the brown scale indicates faster rate of change in the extreme, while the blue scales indicates faster rate of change in the central trend. **b,** trends of change in regions with the highest and lowest values of differences between the slope of change of central and extreme percentiles. The region with the 10% highest values is where the extreme slopes of change are greater than the central slopes of change and vice-versa. Graphs show the trends of change in mean and maximum temperature, VPD and temperature-linked MCWD from 1981 to 2023 in both regions. Lines represent the median curves for 5th, 50th and 95th percentiles and shaded areas around the lines represent the interquartile range (IQR) +/- 25% - i.e., the dispersion of 50% of all curves.

Linking climate change to historical averages and land use change

Given the strong spatial signal of the observed climate trends, we investigated whether central or extreme trends were spatially associated with the historical averages from the start of the time series (1981–1990; Extended Data Figure S10). The data were variable across metrics, and most correlation coefficients were generally non-significant (Extended Data Figure S10a). However, central trends were more positively associated with historical averages than the extreme trends, and there was a significant positive internal association between rates of change at the 50th percentile and the historical climate for $MCWD_{Temp}$ ($r = 0.37$) and for VPD measured across the hydrological year ($r = 0.27$) and in the driest period ($r = 0.34$). These associations indicate that regions with historically higher MCWD and VPD values are experiencing the highest rates of change for central trends.

The Amazon has been at the forefront of deforestation and land use change over the past 50 years, with a loss of 17% of its original native vegetation since 1985 – the vast majority of which has been converted to agricultural land (70.8% pastures, 17.2% croplands and 12.0% other uses) (MapBiomas, 2025). The central trends of temperature, VPD and $MCWD_{Temp}$ were weakly associated with the present-day distribution of agricultural land ($r = 0.09$-0.32) highlighting deforestation's contribution to changing temperatures in Amazonia (Franco et al., 2025). However, extreme trends had little or no association with the present-day distribution of agricultural land (Extended Data Figure S10b, Figure 2, Figure 3) suggesting global climate change is the primary driver of change in the central-north region.

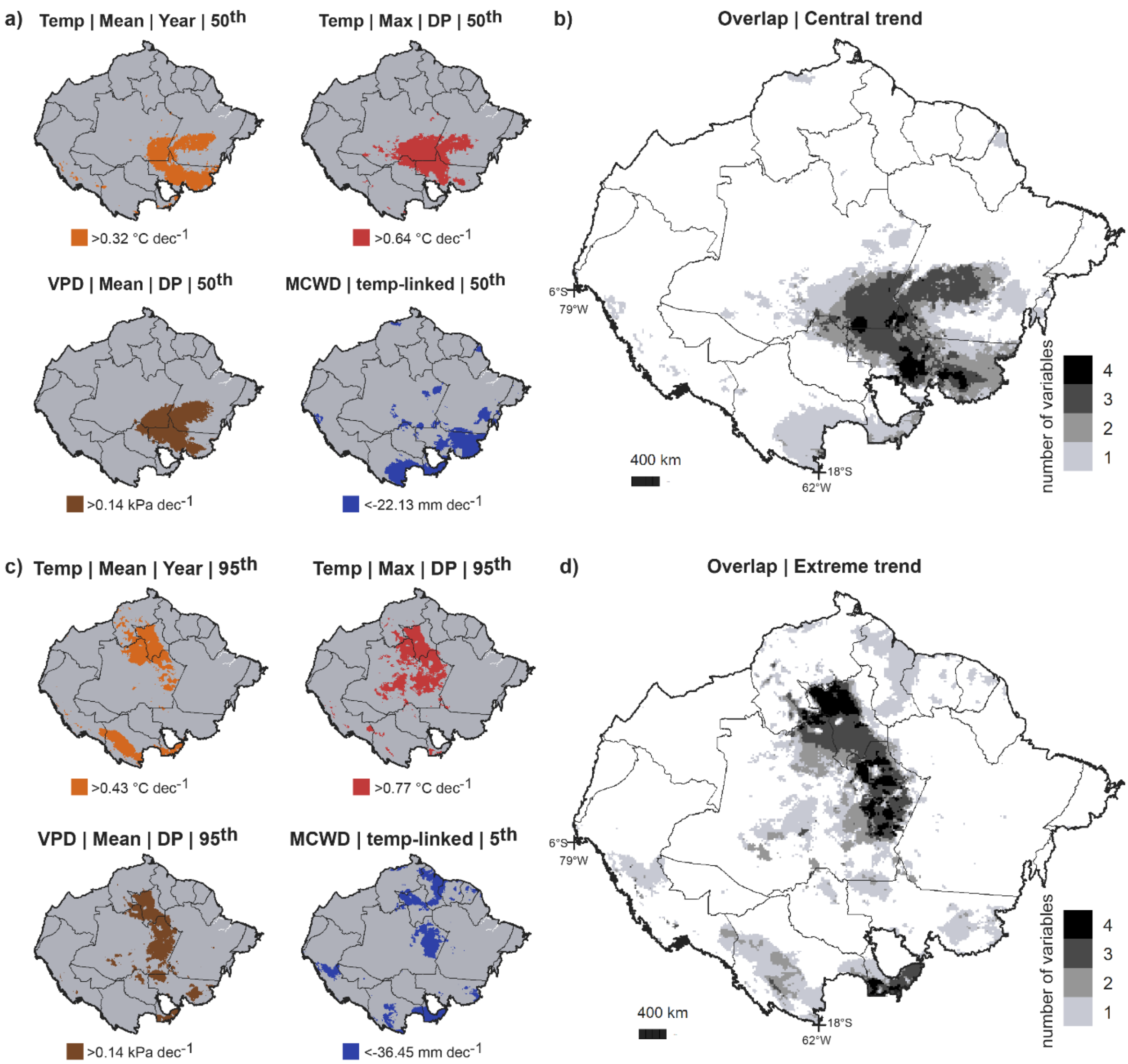

Figure 4. Critical areas with the highest rate of change in the central trend and extremes. Regions within the 10% top values of decadal rate of change in the **a,** central trend and **b,** extreme (95th percentile for mean temperature in the hydrological year, maximum temperature and mean vapour-pressure deficit (VPD) both in the driest period (DP); 5th percentile for maximum cumulative water deficit (MCWD) with temperature-linked. **c,** Overlap of all variables for central trend and **d,** extremes, ranging from one to four overlapping variables.

Discussion

Amazonia's climate, affected by global and regional anthropogenic pressures, has changed rapidly, but not uniformly. Extremes are changing at a much higher rate than central trends and Amazonia wide shifts in temperature – rather than precipitation – are driving most of the changes in water deficit and VPD. Crucially, we identified a hitherto under-emphasised and spatially distinct region of high climate change. While the southern Amazon is confirmed as the fastest warming region on average, it is the central-northern region that is experiencing the greatest rates of increase in extreme temperature and VPD.

This central-northern region is a critical part of Amazonia's cultural and biological wealth, encompassing extensive areas of high forest cover, native savannas, and key indigenous territories, including the Coata-Laranjal, Waimiri-Atroari, Yanomami and Trombetas/Mapuera (Extended Data Figure S9). The historical record of maximum temperatures (Extended Data Figure S4) and water deficit (Extended Data S6) suggest this region could be less adapted to hotter or drier conditions than forests in south and eastern Amazonia. Multiple lines of evidence demonstrate that climate extremes are already affecting socio-ecological systems in this area. Examples include the first observed mass mortality of forest mammals in Amazonia (Guimaraes et al., 2025) and the loss of understorey bird populations and changes in bird lifespans, behaviour and morphology (Avilla et al., 2021; Jirinec et al., 2021; Wolfe et al., 2025). Aquatic systems have undergone extreme reductions in surface water (Souza Jr et al., 2024) and abrupt shifts in fish assemblages (Röpke et al., 2017). Extreme heat and water deficit have contributed to extensive forest fires in the Brazilian state of Roraima (Xaud et al., 2013) and in flooded forests along the Rio Negro (Carvalho et al., 2021b). These and other fire events have likely contributed to record levels of air pollution and hospitalisations in the largest Amazonian urban centre of Manaus (Smith et al., 2014; Tadano et al., 2024).

The drivers of the increase in extremes in the central-northern region require further investigation. The record drought of 2023/24 provides insights, as the low rainfall and high temperatures in the northern Amazon were linked to sea surface temperature (SST) anomalies in the eastern tropical and central equatorial Pacific relating to the transition from La Niña to El Niño conditions (Espinoza et al., 2024). The region has also been identified as being at risk from major global climatic events, such as a slowing down of the Atlantic Meridional Overturning Circulation (AMOC) (Akabane et al., 2024) or changes in cloud cover linked to a narrowing of the Inter Tropical Convergence Zone (Tselioudis et al., 2025). However, the extent of these changes remains uncertain (Terhaar et al., 2025; Voosen, 2025). Changes in soil moisture have been shown to exert a strong influence on extreme temperatures in regional hotspots of warming (Berg et al., 2014), but much of the central-northern region has experienced increases in annual and dry-period precipitation (Extended Data Figure S7) and soils are variable and not consistently different from those in regions where extremes have changed less (Quesada et al., 2011). Finally, although land use change has also been linked to changes in climate (Franco et al., 2025; Smith et al., 2023), the extreme trends are less associated with deforestation extent than the central trends (Extended Data Figure S10b).

Regardless of the underlying cause, the high rate of increase of extreme temperatures, VPD and water deficits demonstrates the critical importance of preventing further frontier advance in this region. Additional deforestation would amplify temperature changes and expose the remaining forests to heightened fire risks exacerbated by edge creation, within-forest disturbances such as logging, and the spread of ignition sources (Barlow et al., 2020; Lapola et al., 2023). Sustained investment in adaptation will be required (Lapola et al., 2018), particularly where preexisting infrastructure and development deficiencies exacerbate people's vulnerability and the risks to health (Andrade et al., 2021), wellbeing in urban environments (Campanharo et al., 2022; Tadano et al., 2024), and the viability of sustainable socio-bioeconomies (Evangelista-Vale et al., 2021; Tregidgo et al., 2020). Support will also be required to maintain the viability of some of the key climate change and conservation interventions, as the increase in extreme climate conditions jeopardises both protected areas through megafires (Spínola et al., 2020) and the regrowth of secondary forests (Elias et al., 2020; Heinrich et al., 2021). All of this will require improvements in monitoring to evaluate risks and identify the most effective adaptation approaches.

There was no clear signal of strong reductions of precipitation across Amazonia, or major differences between central and extreme trends. The only region where rainfall declined significantly in our analysis (Extended Data Figure S7) and in other studies (Flores et al., 2024) was small and bisected the Brazilian states of Rondônia and Amazonas. In fact, overall, there was a slight increase in biome wide averages. This could reflect increased moisture arriving from the warming tropical Atlantic Ocean (Beveridge et al., 2024; Espinoza et al., 2018; Gloor et al., 2013) acting to offset the local and regional losses of precipitation resulting from deforestation (Franco et al., 2025; Smith et al., 2023). The lack of a wider decline of rainfall in southern Amazonia contrasts with research based on rainfall gauges and other rainfall reanalysis products that identify a strong and consistent drying signal across a similar period (Fu et al., 2013; Marengo et al., 2022). Although satellite products can underestimate periods of high rainfall and dry days (Cordeiro & Blanco, 2021), CHIRPS is considered one of is the best products for tropical precipitation during extreme climate events (Burton et al., 2018) and is even more accurate in drier regions of the Amazon (Cordeiro & Blanco, 2021) where the greatest drying trend has been identified in other studies (Marengo et al., 2022). Furthermore, the overall increase in rainfall detected by CHIRPS is consistent with increased river flows (Gloor et al., 2013) and ground water storage (Heerspink et al., 2020). In contrast, the signal from rainfall gauges used in previous work (Fu et al., 2013) is difficult to interpret due to their sparse coverage (Zhao & Ma, 2019), inconsistent directional trends across stations (Cattelan et al., 2025; Paca et al., 2020), and their biased distribution towards the most deforested areas (Mu and Jones 2022) and along rivers where the breeze influences rainfall (Fitzjarrald et al., 2008). Such divergences highlight the importance of improving the observational network across tropical South America (Cattelan et al., 2025).

Overall, changes in temperature rather than precipitation are driving the most significant increases in VPD and reductions in $MCWD_{Temp}$, with the highest recorded changes in the central-north region occurring where there is a good coverage of weather stations (Cattelan et al., 2025) to inform and constrain climate reanalysis data. However, the large difference between our temperature-invariant and temperature-linked measures of water deficit highlights the urgent need to reduce uncertainty around temperature and CO_2 effects on evapotranspiration in tropical forests. Elevated CO_2 induces stomatal closure, causing plants to reduce transpiration under elevated CO_2 (Cernusak et al., 2013; De Kauwe et al., 2013). Malhi et al., (2009) predict this reduction would be smaller than the temperature-induced increases in evaporation from the soil or transpiration from the leaf. Although other models suggest a stronger influence of CO_2 than temperature (Richardson et al., 2018), an overall increase in evapotranspiration is consistent with the relationship between temperature and potential evapotranspiration in the Penman-Monteith model (Song et al., 2023) and from models and remote sensing observations conducted across the arc of deforestation (Laipelt et al., 2025). Furthermore, our use of 8.9 mm for every degree increase in temperature (Malhi et al., 2009) is potentially very conservative compared to the observed 11% increase in dry season ET over the arc of deforestation over 23 years, when mean temperatures increased by c. 0.50 ºC (Figure 2) and where a higher increase in ET was offset by forest loss (Laipelt et al., 2025). However, many uncertainties remain as changes in evapotranspiration are likely to be spatially variable (Heerspink et al., 2020), will vary across years and seasons (Malhi et al., 2009), and may be sensitive to forest disturbances (Longo et al., 2025).

We show that climate change in Amazonia is neither gradual nor homogenous, and that public policies must address the enormous challenge of rapidly increasing extreme temperatures and water deficits. Crucially, these are occurring in the central-northern region, far from the arc of deforestation. This spatial dissociation with forest loss – the main local driver of climate change (Franco et al., 2025) – demonstrates that the world's highest greenhouse emitting countries bear a strong responsibility for Amazonia's rapidly changing socio-ecological condition. This underscores once again the urgent need for rapid reductions in greenhouse gas emissions (Dosio et al., 2018) and strengthens arguments that high emitting countries should contribute to adaptation and conservation interventions in tropical forest regions through mechanisms such as the Fund for responding to Loss and Damage or novel initiatives such as the Tropical Forest

Forever Facility. It is vital that this support reaches the most vulnerable regions and peoples and prevents any further frontier advance that could amplify the consequences of climate extremes.

Acknowledgements

We thank WWF-UK for funding the core analysis, alongside additional support from UKRI's Amazon-SOS (NE/X019039/1) and Rainfauna (NE/X015262/1) projects, BNP Paribas Foundation's Climate and Biodiversity initiative, DEFRA's Global Centre for Biodiversity and Climate, and CNPq's Centro Avançado em Pesquisas Socioecológicas para a Recuperação Ambiental da Amazônia (CAPOEIRA - 352886/2025-0) and PELD (445994/2024-0). LMM acknowledges funding from the UK Natural Environment Research Council (NERC) projects NE/X001172/1 and NE/W004895/1.

Author contributions

JB and MB conceived the paper. NC and CAN analysed the data, with additional input from CHLSJ. JB, NC and CAN led the writing of the manuscript. All authors contributed to the development of the analysis, the interpretation of results and the writing of the manuscript.

Competing interests

The authors declare no competing financial interests.

Data and Code availability

The data and the code will be available in Zenodo once the paper is accepted for publication.

References

Akabane, T. K., Chiessi, C. M., Hirota, M., Bouimetarhan, I., Prange, M., Mulitza, S., Bertassoli, D. J., Häggi, C., Staal, A., Lohmann, G., Boers, N., Daniau, A. L., Oliveira, R. S., Campos, M. C., Shi, X., & De Oliveira, P. E. (2024). Weaker Atlantic overturning circulation increases the vulnerability of northern Amazon forests. *Nature Geoscience*, *17*(12), 1284–1290. https://doi.org/10.1038/s41561-024-01578-z

Alencar, A., Brando, P. M., Asner, G. P., & Putz, F. E. (2015). Landscape Fragmentation, Severe Drought and the New Amazon Forest Fire Regime. *Ecological Society of America*, *25*(6), 1493–1505.

Andrade, L. de M. B., Guedes, G. R., de Souza Noronha, K. V. M., Silva, C. M. S., Andrade, J. P., & Martins, A. S. F. S. (2021). Health-related vulnerability to climate extremes in homoclimatic zones of Amazonia and Northeast region of Brazil. *PLoS ONE*, *16*(11 November 2021). https://doi.org/10.1371/journal.pone.0259780

Aragão, L. E. O. C., Anderson, L. O., Fonseca, M. G., Rosan, T. M., Vedovato, L. B., Wagner, F. H., Silva, C. V. J., Silva Junior, C. H. L., Arai, E., Aguiar, A. P., Barlow, J., Berenguer, E., Deeter, M. N., Domingues, L. G., Gatti, L., Gloor, M., Malhi, Y., Marengo, J. A., Miller, J. B., ... Saatchi, S. (2018). 21st Century drought-related fires counteract the decline of Amazon deforestation carbon emissions. *Nature Communications*, *9*(1). https://doi.org/10.1038/s41467-017-02771-y

Aragão, L. E. O. C., Malhi, Y., Roman-Cuesta, R. M., Saatchi, S., Anderson, L. O., & Shimabukuro, Y. E. (2007). Spatial patterns and fire response of recent Amazonian droughts. *Geophysical Research Letters*, *34*(7). https://doi.org/10.1029/2006GL028946

Avilla, S. S., Sieving, K. E., Anciães, M., & Cornelius, C. (2021). Phenotypic variation in a neotropical understory bird driven by environmental change in an urbanizing Amazonian landscape. *Oecologia*, *196*(3), 763–779. https://doi.org/10.1007/s00442-021-04976-x

Barlow, J., Berenguer, E., Carmenta, R., & França, F. (2020). Clarifying Amazonia's burning crisis. In *Global Change Biology* (Vol. 26, Issue 2, pp. 319–321). Blackwell Publishing Ltd. https://doi.org/10.1111/gcb.14872

Barlow, J., França, F., Gardner, T. A., Hicks, C. C., Lennox, G. D., Berenguer, E., Castello, L., Economo, E. P., Ferreira, J., Guénard, B., Gontijo Leal, C., Isaac, V., Lees, A. C., Parr, C. L., Wilson, S. K., Young, P. J., & Graham, N. A. J. (2018). The future of hyperdiverse tropical ecosystems. In *Nature* (Vol. 559, Issue 7715, pp. 517–526). Nature Publishing Group. https://doi.org/10.1038/s41586-018-0301-1

Bennett, A. C., Rodrigues de Sousa, T., Monteagudo-Mendoza, A., Esquivel-Muelbert, A., Morandi, P. S., Coelho de Souza, F., Castro, W., Duque, L. F., Flores Llampazo, G., Manoel dos Santos, R., Ramos, E., Vilanova Torre, E., Alvarez-Davila, E., Baker, T. R., Costa, F. R. C., Lewis, S. L., Marimon, B. S., Schietti, J., Burban, B., ... Phillips, O. L. (2023). Sensitivity of South American tropical forests to an extreme climate anomaly. *Nature Climate Change*, *13*(9), 967–974. https://doi.org/10.1038/s41558-023-01776-4

Berenguer, E., Lennox, G. D., Ferreira, J., Malhi, Y., Aragão, L. E. O. C., Barreto, J. R., Espírito-Santo, F. D. B., Figueiredo, A. E. S., França, F., Gardner, T. A., Joly, C. A., Palmeira, A. F., Quesada, C. A., Rossi, L. C., de Seixas, M. M. M., Smith, C. C., Withey, K., & Barlow, J. (2021). Tracking the impacts of El Niño drought and fire in human-modified Amazonian forests. *Proceedings of the National Academy of Sciences of the United States of America*, *118*(30), e2019377118. https://doi.org/10.1073/pnas.2019377118/-/DCSupplemental

Berg, A., Lintner, B. R., Findell, K. L., Malyshev, S., Loikith, P. C., & Gentine, P. (2014). Impact of soil moisture-atmosphere interactions on surface temperature distribution. *Journal of Climate*, *27*(21), 7976–7993. https://doi.org/10.1175/JCLI-D-13-00591.1

Beveridge, C. F., Espinoza, J. C., Athayde, S., Correa, S. B., Couto, T. B. A., Heilpern, S. A., Jenkins, C. N., Piland, N. C., Utsunomiya, R., Wongchuig, S., & Anderson, E. P. (2024). The Andes–Amazon–Atlantic pathway: A foundational hydroclimate system for social–ecological system sustainability. *Proceedings of the National Academy of Sciences of the United States of America*, *121*(22). https://doi.org/10.1073/pnas.2306229121

Brando, P. M., Balch, J. K., Nepstad, D. C., Morton, D. C., Putz, F. E., Coe, M. T., Silvério, D., Macedo, M. N., Davidson, E. A., Nóbrega, C. C., Alencar, A., & Soares-Filho, B. S. (2014). Abrupt increases in Amazonian tree mortality due to drought-fire interactions. *Proceedings of the National Academy of Sciences of the United States of America*, *111*(17), 6347–6352. https://doi.org/10.1073/pnas.1305499111

Brando, P. M., Barlow, J., Macedo, M. N., Silvério, D. V, Ferreira, J. N., Maracahipes, L., Anderson, L., Morton, D. C., Alencar, A., Paolucci, L. N., Jacobs, S., Stouter, H., Randerson, J., Flores, B. M., Starinchak, B., Coe, M., Pires, M. M., Rattis, L., Armenteras, D., ... Uribe, M. (2025). *Annual Review of Environment and Resources Tipping Points of Amazonian Forests: Beyond Myths and Toward Solutions*. *247*, 17. https://doi.org/10.1146/annurev-environ-111522

Burton, C., Rifai, S., & Malhi, Y. (2018). Inter-comparison and assessment of gridded climate products over tropical forests during the 2015/2016 El Niño. *Philosophical Transactions of the Royal Society B: Biological Sciences*, *373*(1760). https://doi.org/10.1098/rstb.2017.0406

Campanharo, W. A., Morello, T., Christofoletti, M. A. M., & Anderson, L. O. (2022). Hospitalization due to fire-induced pollution in the brazilian legal amazon from 2005 to 2018. *Remote Sensing*, *14*(1). https://doi.org/10.3390/rs14010069

Carvalho, N. S., Anderson, L. O., Nunes, C. A., Pessôa, A. C. M., Silva Junior, C. H. L., Reis, J. B. C., Shimabukuro, Y. E., Berenguer, E., Barlow, J., & Aragão, L. E. O. C. (2021). Spatio-Temporal variation in dry season determines the Amazonian fire calendar. *Environmental Research Letters*, *16*(12). https://doi.org/10.1088/1748-9326/ac3aa3

Carvalho, T. C., Wittmann, F., Piedade, M. T. F., Resende, A. F. de, Silva, T. S. F., & Schöngart, J. (2021). Fires in Amazonian Blackwater Floodplain Forests: Causes, Human Dimension, and Implications for Conservation. *Frontiers in Forests and Global Change*, *4*. https://doi.org/10.3389/ffgc.2021.755441

Cattelan, L. G., Mattos, C. R. C., & Hirota, M. (2025). Unraveling divergences: disagreement between precipitation datasets and stations in tropical South America. *Environmental Research Letters* , *20*(10). https://doi.org/10.1088/1748-9326/ae02aa

Cernusak, L. A., Ubierna, N., Winter, K., Holtum, J. A. M., Marshall, J. D., & Farquhar, G. D. (2013). Environmental and physiological determinants of carbon isotope discrimination in terrestrial plants. In *New Phytologist* (Vol. 200, Issue 4, pp. 950–965). https://doi.org/10.1111/nph.12423

Cordeiro, A. L. de M., & Blanco, C. J. C. (2021). Assessment of satellite products for filling rainfall data gaps in the Amazon region. *Natural Resource Modeling*, *34*(2). https://doi.org/10.1111/nrm.12298

De Kauwe, M. G., Medlyn, B. E., Zaehle, S., Walker, A. P., Dietze, M. C., Hickler, T., Jain, A. K., Luo, Y., Parton, W. J., Prentice, I. C., Smith, B., Thornton, P. E., Wang, S., Wang, Y. P., Wårlind, D., Weng, E., Crous, K. Y., Ellsworth, D. S., Hanson, P. J., ... Norby, R. J. (2013). Forest water use and water use efficiency at elevated CO2: A model-data intercomparison at two contrasting temperate forest FACE sites. *Global Change Biology*, *19*(6), 1759–1779. https://doi.org/10.1111/gcb.12164

Dosio, A., Mentaschi, L., Fischer, E. M., & Wyser, K. (2018). Extreme heat waves under 1.5 °c and 2 °c global warming. *Environmental Research Letters*, *13*(5). https://doi.org/10.1088/1748-9326/aab827

Ebi, K. L., Vanos, J., Baldwin, J. W., Bell, J. E., Hondula, D. M., Errett, N. A., Hayes, K., Reid, C. E., Saha, S., Spector, J., & Berry, P. (2020). Extreme Weather and Climate Change: Population

Health and Health System Implications. In *Annual Review of Public Health* (Vol. 42, pp. 293–315). Annual Reviews Inc. https://doi.org/10.1146/annurev-publhealth-012420-105026

Elias, F., Ferreira, J., Lennox, G. D., Berenguer, E., Ferreira, S., Schwartz, G., Melo, L. de O., Reis Júnior, D. N., Nascimento, R. O., Ferreira, F. N., Espirito-Santo, F., Smith, C. C., & Barlow, J. (2020). Assessing the growth and climate sensitivity of secondary forests in highly deforested Amazonian landscapes. *Ecology*, *101*(3). https://doi.org/10.1002/ecy.2954

Espinoza, J. C., Jimenez, J. C., Marengo, J. A., Schongart, J., Ronchail, J., Lavado-Casimiro, W., & Ribeiro, J. V. M. (2024). The new record of drought and warmth in the Amazon in 2023 related to regional and global climatic features. *Scientific Reports*, *14*(1). https://doi.org/10.1038/s41598-024-58782-5

Espinoza, V., Waliser, D. E., Guan, B., Lavers, D. A., & Ralph, F. M. (2018). Global Analysis of Climate Change Projection Effects on Atmospheric Rivers. *Geophysical Research Letters*, *45*(9), 4299–4308. https://doi.org/10.1029/2017GL076968

Evangelista-Vale, J. C., Weihs, M., José-Silva, L., Arruda, R., Sander, N. L., Gomides, S. C., Machado, T. M., Pires-Oliveira, J. C., Barros-Rosa, L., Castuera-Oliveira, L., Matias, R. A. M., Martins-Oliveira, A. T., Bernardo, C. S. S., Silva-Pereira, I., Carnicer, C., Carpanedo, R. S., & Eisenlohr, P. V. (2021). Climate change may affect the future of extractivism in the Brazilian Amazon. *Biological Conservation*, *257*. https://doi.org/10.1016/j.biocon.2021.109093

Fitzjarrald, D. R., Sakai, R. K., Moraes, O. L. L., De Oliveira, R. C., Acevedo, O. C., Czikowsky, M. J., & Beldini, T. (2008). Spatial and temporal rainfall variability near the amazon-tapajós confluence. *Journal of Geophysical Research: Biogeosciences*, *114*(1). https://doi.org/10.1029/2007JG000596

Flores, B. M., Montoya, E., Sakschewski, B., Nascimento, N., Staal, A., Betts, R. A., Levis, C., Lapola, D. M., Esquível-Muelbert, A., Jakovac, C., Nobre, C. A., Oliveira, R. S., Borma, L. S., Nian, D., Boers, N., Hecht, S. B., ter Steege, H., Arieira, J., Lucas, I. L., … Hirota, M. (2024). Critical transitions in the Amazon forest system. *Nature*, *626*(7999), 555–564. https://doi.org/10.1038/s41586-023-06970-0

Franco, M. A., Rizzo, L. V., Teixeira, M. J., Artaxo, P., Azevedo, T., Lelieveld, J., Nobre, C. A., Pöhlker, C., Pöschl, U., Shimbo, J., Xu, X., & Machado, L. A. T. (2025). How climate change and deforestation interact in the transformation of the Amazon rainforest. *Nature Communications*, *16*(1), 7944. https://doi.org/10.1038/s41467-025-63156-0

Fu, R., Yin, L., Li, W., Arias, P. A., Dickinson, R. E., Huang, L., Chakraborty, S., Fernandes, K., Liebmann, B., Fisher, R., & Myneni, R. B. (2013). Increased dry-season length over southern Amazonia in recent decades and its implication for future climate projection. *Proceedings of the National Academy of Sciences of the United States of America*, *110*(45), 18110–18115. https://doi.org/10.1073/pnas.1302584110

Gatti, L. V., Basso, L. S., Miller, J. B., Gloor, M., Gatti Domingues, L., Cassol, H. L. G., Tejada, G., Aragão, L. E. O. C., Nobre, C., Peters, W., Marani, L., Arai, E., Sanches, A. H., Corrêa, S. M., Anderson, L., Von Randow, C., Correia, C. S. C., Crispim, S. P., & Neves, R. A. L. (2021). Amazonia as a carbon source linked to deforestation and climate change. *Nature*, *595*(7867), 388–393. https://doi.org/10.1038/s41586-021-03629-6

Gloor, M., Brienen, R. J. W., Galbraith, D., Feldpausch, T. R., Schöngart, J., Guyot, J. L., Espinoza, J. C., Lloyd, J., & Phillips, O. L. (2013). Intensification of the Amazon hydrological cycle over the last two decades. *Geophysical Research Letters*, *40*(9), 1729–1733. https://doi.org/10.1002/grl.50377

Guimaraes, A. F., Schietti, J., Querido, L. C. A., Nunes, J., Santos, P., Lagroteria, D., & Gordo, M. (2025). Extreme drought and heat lead to alarming mortality of Amazon fauna. *Acta Amazonica*, *55*. https://doi.org/10.1590/1809-4392202404053

Heerspink, B. P., Kendall, A. D., Coe, M. T., & Hyndman, D. W. (2020). Trends in streamflow, evapotranspiration, and groundwater storage across the Amazon Basin linked to changing precipitation and land cover. *Journal of Hydrology: Regional Studies*, *32*. https://doi.org/10.1016/j.ejrh.2020.100755

Heinrich, V. H. A., Dalagnol, R., Cassol, H. L. G., Rosan, T. M., de Almeida, C. T., Silva Junior, C. H. L., Campanharo, W. A., House, J. I., Sitch, S., Hales, T. C., Adami, M., Anderson, L. O., & Aragão, L. E. O. C. (2021). Large carbon sink potential of secondary forests in the Brazilian Amazon to mitigate climate change. *Nature Communications*, *12*(1). https://doi.org/10.1038/s41467-021-22050-1

Huntingford, C., Cox, P. M., Ritchie, P. D. L., Clarke, J. J., Parry, I. M., & Williamson, M. S. (2024). Acceleration of daily land temperature extremes and correlations with surface energy fluxes. *Npj Climate and Atmospheric Science*, *7*(1). https://doi.org/10.1038/s41612-024-00626-0

IPCC, I. P. on C. C. G., McLeman, R., Adams, H., Aldunce, P., Bowen, K., Campbell-Lendrum, D., Clayton, S., Ebi, K. L., Hess, J., Huang, C., Liu, Q., McGregor, G., Semenza, J., & Tirado, M. C. (2022). Health, Wellbeing and the Changing Structure of Communities. In H.-O. Pörtner, D. C. Roberts, M. M. B. Tignor, E. S. Poloczanska, K. Mintenbeck, A. Alegría, M. Craig, S. Langsdorf, S. Löschke, V. Möller, A. E. Okem, & B. Rama (Eds.), *Health, Wellbeing, and the Changing Structure of Communities. In: Climate Change 2022: Impacts, Adaptation and Vulnerability. Contribution of Working Group II to the Sixth Assessment Report of the Intergovernmental Panel on Climate Change* (pp. 1041–1170). Cambridge University Press. https://doi.org/10.1017/9781009325844.009

Jiménez-Muñoz, J. C., Sobrino, J. A., Mattar, C., & Malhi, Y. (2013). Spatial and temporal patterns of the recent warming of the Amazon forest. *Journal of Geophysical Research Atmospheres*, *118*(11), 5204–5215. https://doi.org/10.1002/jgrd.50456

Jirinec, V., Burner, R. C., Amaral, B. R., Bierregaard Jr, R. O., Fernández-Arellano, G., Hernández-Palma, A., Johnson, E. I., Lovejoy, T. E., Powell, L. L., Rutt, C. L., Wolfe, J. D., & Stouffer, P. C. (2021). Morphological consequences of climate change for resident birds in intact Amazonian rainforest. In *Sci. Adv* (Vol. 7). https://www.science.org

Kotz, M., Amano, T., & Watson, J. E. M. (2025). Large reductions in tropical bird abundance attributable to heat extreme intensification. *Nature Ecology & Evolution*. https://doi.org/10.1038/s41559-025-02811-7

Laipelt, L., Fleischmann, A., de Andrade, B. C., Vergopolan, N., Biudes, M. S., Aragão, L. E. O. C., Collischonn, W., & Ruhoff, A. (2025). Increased Amazon evapotranspiration since 1990 in a warming climate. *Environmental Research Letters* , *20*(10). https://doi.org/10.1088/1748-9326/adfc00

Lapola, D. M., Pinho, P., Barlow, J., Aragão, L. E. O. C., Berenguer, E., Carmenta, R., Liddy, H. M., Seixas, H., Silva, C. V. J., Silva, C. H. L., Alencar, A. A. C., Anderson, L. O., Armenteras, D., Brovkin, V., Calders, K., Chambers, J., Chini, L., Costa, M. H., Faria, B. L., … Walker, W. S. (2023). The drivers and impacts of Amazon forest degradation. In *Science* (Vol. 379, Issue 6630). American Association for the Advancement of Science. https://doi.org/10.1126/science.abp8622

Lapola, D. M., Pinho, P., Quesada, C. A., Strassburg, B. B. N., Rammig, A., Kruijt, B., Brown, F., Ometto, J. P. H. B., Premebida, A., Jos ´, J., Marengo, J. A., Vergara, W., & Nobre, C. A. (2018). *Limiting the high impacts of Amazon forest dieback with no-regrets science and policy action*. https://doi.org/10.1073/pnas.1721770115/-/DCSupplemental

Libonati, R., Geirinhas, J. L., Silva, P. S., Monteiro dos Santos, D., Rodrigues, J. A., Russo, A., Peres, L. F., Narcizo, L., Gomes, M. E. R., Rodrigues, A. P., DaCamara, C. C., Pereira, J. M. C., & Trigo, R. M. (2022). Drought–heatwave nexus in Brazil and related impacts on health and fires: A comprehensive review. In *Annals of the New York Academy of Sciences* (Vol. 1517, Issue 1, pp. 44–62). John Wiley and Sons Inc. https://doi.org/10.1111/nyas.14887

Lima, L. S. de, Silva, F. E. O. e., Dorio Anastácio, P. R., Kolanski, M. M. de P., Pires Pereira, A. C., Menezes, M. S. R., Cunha, E. L. T. P., & Macedo, M. N. (2024). Severe droughts reduce river navigability and isolate communities in the Brazilian Amazon. *Communications Earth and Environment*, *5*(1). https://doi.org/10.1038/s43247-024-01530-4

Longo, M., Keller, M., Kueppers, L. M., Bowman, K. W., Csillik, O., Ferraz, A., Moorcroft, P. R., Ometto, J. P., Soares-Filho, B. S., Xu, X., de Assis, M. L. R., Görgens, E. B., Larson, E. J. L., Needham, J. F., Ordway, E. M., Pereira, F. R. S., Rangel Pinagé, E., Sato, L., Xu, L., & Saatchi, S. (2025). Degradation and deforestation increase the sensitivity of the amazon forest to climate extremes. *Environmental Research Letters* , *20*(5). https://doi.org/10.1088/1748-9326/adc58c

Machado-Silva, F., Libonati, R., Melo de Lima, T. F., Bittencourt Peixoto, R., de Almeida França, J. R., de Avelar Figueiredo Mafra Magalhães, M., Lemos Maia Santos, F., Abrantes Rodrigues, J., & DaCamara, C. C. (2020). Drought and fires influence the respiratory diseases hospitalizations in the Amazon. *Ecological Indicators*, *109*. https://doi.org/10.1016/j.ecolind.2019.105817

Malhi, Y., Aragão, L. E. O. C., Galbraith, D., Huntingford, C., Fisher, R., Zelazowski, P., Sitch, S., McSweeney, C., & Meir, P. (2009). Exploring the likelihood and mechanism of a climate-change-induced dieback of the Amazon rainforest. *Proceedings of the National Academy of Sciences of the United States of America*, *106*(49), 20610–20615. https://doi.org/https://doi.org/10.1073/pnas.0804619106

MapBiomas. (2025). *MapBiomas Amazonian Project - Collection 6 of the Annual Land Use and Land Cover Maps of Amazonian, accessed on 12 January through the link: [https://amazonia.mapbiomas.org/en/mapbiomas-amazonia-collection/]*. https://mapbiomas.org/

Marengo, J. A., Espinoza, J. C., Fu, R., Jimenez Muñoz, J. C., Alves, L. M., DA ROCHA, H. R., & Schöngart, J. (2024). Long-term variability, extremes and changes in temperature and hydrometeorology in the Amazon region: A review. *Acta Amazonica*, *54*(spe1). https://doi.org/10.1590/1809-4392202200980

Marengo, J. A., Jimenez, J. C., Espinoza, J. C., Cunha, A. P., & Aragão, L. E. O. (2022). Increased climate pressure on the agricultural frontier in the Eastern Amazonia–Cerrado transition zone. *Scientific Reports*, *12*(1). https://doi.org/10.1038/s41598-021-04241-4

Maxwell, S. L., Butt, N., Maron, M., McAlpine, C. A., Chapman, S., Ullmann, A., Segan, D. B., & Watson, J. E. M. (2018). Conservation implications of ecological responses to extreme weather and climate events. In *Diversity and Distributions* (Vol. 25, Issue 4, pp. 613–625). Blackwell Publishing Ltd. https://doi.org/10.1111/ddi.12878

Paca, V. H. da M., Espinoza-Dávalos, G. E., Moreira, D. M., & Comair, G. (2020). Variability of trends in precipitation across the Amazon river basin determined from the CHIRPS precipitation product and from station records. *Water (Switzerland)*, *12*(5). https://doi.org/10.3390/W12051244

Qin, Y., Wang, D., Ziegler, A. D., Fu, B., & Zeng, Z. (2025). Impact of Amazonian deforestation on precipitation reverses between seasons. *Nature*, *639*(8053), 102–108. https://doi.org/10.1038/s41586-024-08570-y

Quesada, C. A., Lloyd, J., Anderson, L. O., Fyllas, N. M., Schwarz, M., & Czimczik, C. I. (2011). Soils of Amazonia with particular reference to the RAINFOR sites. *Biogeosciences*, *8*(6), 1415–1440. https://doi.org/10.5194/bg-8-1415-2011

Ray, D., Nepstad, D., & Moutinho, P. (2005). Micrometeorological and canopy controls of fire susceptibility in a forested Amazon landscape. *Ecological Applications*, *15*(5), 1664–1678. https://doi.org/10.1890/05-0404

Richardson, T. B., Forster, P. M., Andrews, T., Boucher, O., Faluvegi, G., Fläschner, D., Kasoar, M., Kirkevåg, A., Lamarque, J. F., Myhre, G., Olivié, D., Samset, B. H., Shawki, D., Shindell, D., Takemura, T., & Voulgarakis, A. (2018). Carbon Dioxide Physiological Forcing Dominates Projected Eastern Amazonian Drying. *Geophysical Research Letters*, *45*(6), 2815–2825. https://doi.org/10.1002/2017GL076520

Röpke, C. P., Amadio, S., Zuanon, J., Ferreira, E. J. G., De Deus, C. P., Pires, T. H. S., & Winemiller, K. O. (2017). Simultaneous abrupt shifts in hydrology and fish assemblage structure in a floodplain lake in the central Amazon. *Scientific Reports*, *7*. https://doi.org/10.1038/srep40170

Silva Junior, C. H. L., Anderson, L. O., Silva, A. L., Almeida, C. T., Dalagnol, R., Pletsch, M. A. J. S., Penha, T. V., Paloschi, R. A., & Aragão, L. E. O. C. (2019). Fire responses to the 2010 and 2015/2016 Amazonian droughts. *Frontiers in Earth Science*, *7*, 1–16. https://doi.org/10.3389/feart.2019.00097

Silva Junior, C. H. L., Pessôa, A. C. M., Carvalho, N. S., Reis, J. B. C., Anderson, L. O., & Aragão, L. E. O. C. (2021). The Brazilian Amazon deforestation rate in 2020 is the greatest of the decade. In *Nature Ecology and Evolution* (Vol. 5, Issue 2, pp. 144–145). Nature Research. https://doi.org/10.1038/s41559-020-01368-x

Smith, C., Baker, J. C. A., & Spracklen, D. V. (2023). Tropical deforestation causes large reductions in observed precipitation. *Nature*, *615*(7951), 270–275. https://doi.org/10.1038/s41586-022-05690-1

Smith, L. T., Aragão, L. E. O. C., Sabel, C. E., & Nakaya, T. (2014). Drought impacts on children's respiratory health in the Brazilian Amazon. *Nature Scientific Reports*, *4*(3726), 1–8. https://doi.org/10.1038/srep03726

Song, Y. H., Chung, E. S., Shahid, S., Kim, Y., & Kim, D. (2023). Development of global monthly dataset of CMIP6 climate variables for estimating evapotranspiration. *Scientific Data*, *10*(1). https://doi.org/10.1038/s41597-023-02475-7

Souza Jr, C. M., Marengo, J., Ferreira, B., Ribeiro, J., Schirmbeck, L. W., Schirmbeck, J., Hirye, M., Cunha, A., Wiederhecker, H. C., & Latuf, M. O. (2024). Amazon severe drought in 2023 triggered surface water loss. *Environmental Research: Climate*, *3*(4). https://doi.org/10.1088/2752-5295/ad7c71

Spínola, J. N., Soares da Silva, M. J., Assis da Silva, J. R., Barlow, J., & Ferreira, J. (2020). A shared perspective on managing Amazonian sustainable-use reserves in an era of megafires. *Journal of Applied Ecology*, *57*(11), 2132–2138. https://doi.org/10.1111/1365-2664.13690

Tadano, Y. de S., Potgieter-Vermaak, S., Siqueira, H. V., Hoelzemann, J. J., Duarte, E. S. F., Alves, T. A., Valebona, F., Lenzi, I., Godoi, A. F. L., Barbosa, C., Ribeiro, I. O., de Souza, R. A. F., Yamamoto, C. I., Santos, E., Fernandesi, K. S., Machado, C., Martin, S. T., & Godoi, R. H. M. (2024). Predicting health impacts of wildfire smoke in Amazonas basin, Brazil. *Chemosphere*, *367*. https://doi.org/10.1016/j.chemosphere.2024.143688

Tavares, J. V., Oliveira, R. S., Mencuccini, M., Signori-Müller, C., Pereira, L., Diniz, F. C., Gilpin, M., Marca Zevallos, M. J., Salas Yupayccana, C. A., Acosta, M., Pérez Mullisaca, F. M., Barros, F. de V., Bittencourt, P., Jancoski, H., Scalon, M. C., Marimon, B. S., Oliveras Menor, I., Marimon, B. H., Fancourt, M., … Galbraith, D. R. (2023). Basin-wide variation in tree hydraulic safety margins predicts the carbon balance of Amazon forests. *Nature*, *617*(7959), 111–117. https://doi.org/10.1038/s41586-023-05971-3

Terhaar, J., Vogt, L., & Foukal, N. P. (2025). Atlantic overturning inferred from air-sea heat fluxes indicates no decline since the 1960s. *Nature Communications* , *16*(1). https://doi.org/10.1038/s41467-024-55297-5

Tregidgo, D., Campbell, A. J., Rivero, S., Freitas, M. A. B., & Almeida, O. (2020). Vulnerability of the Açaí Palm to Climate Change. *Human Ecology*, *48*(4), 505–514. https://doi.org/10.1007/s10745-020-00172-2

Tselioudis, G., Remillard, J., Jakob, C., & Rossow, W. B. (2025). Contraction of the World's Storm-Cloud Zones the Primary Contributor to the 21st Century Increase in the Earth's Sunlight Absorption. *Geophysical Research Letters*, *52*(11). https://doi.org/10.1029/2025GL114882

Voosen, P. (2025). Earth's clouds are shrinking, boosting global warming. *Science*, *387*(6729).

Wolfe, J. D., Luther, D. A., Jirinec, V., Collings, J., Johnson, E. I., Bierregaard, R. O., & Stouffer, P. C. (2025). Climate change aggravates bird mortality in pristine tropical forests. In *Sci. Adv* (Vol. 11). https://www.science.org

Xaud, H. A. M., Martins, F. da S. R. V., & Dos Santos, J. R. (2013). Tropical forest degradation by mega-fires in the northern Brazilian Amazon. *Forest Ecology and Management*, *294*, 97–106. https://doi.org/10.1016/j.foreco.2012.11.036

Zhao, H., & Ma, Y. (2019). Evaluating the drought-monitoring utility of four satellite-based quantitative precipitation estimation products at global scale. *Remote Sensing*, *11*(17). https://doi.org/10.3390/rs11172010

Methods

1. Datasets of climate variables

We used the following climate variables and resampling procedures to undertake our assessment of climate change in the Amazon region delimited by (RAISG, 2024).

- Temperature and vapour pressure deficit (VPD): We used ERA5-Land post-processed daily statistics dataset with 1-hour sub-daily frequency sampling over a 44-year period (1981-2024). We use 1981 as the start point to standardise with precipitation data availability, and because 1981 is after the widely-observed change in the rate of climate change that occurred in the 1970s (Burton et al., 2018; Sarkar & Maity, 2021). ERA5-Land is a global climate reanalysis product produced by the European Centre for Medium-Range Weather Forecasts (ECMWF) available at spatial resolution of 0.1° – approximately 11x11 km (Muñoz-Sabater et al., 2021). For temperature metrics, we used the 2-m temperature minimum, mean and maximum daily statistics. We calculated the mean VPD using the '*plantecophys'* R package (Duursma, 2015; R Core Team, 2025), combining the ERA5-Land daily means statistics from 2m temperature, 2m dewpoint and surface pressure.

- Precipitation: We used the daily Rainfall Estimates from Rain Gauge and Satellite Observations (CHIRPS v2) dataset over a 44-year period (1981 to 2024). The CHIRPS algorithm integrates satellite data, ground-based observations and precipitation estimates to produce rainfall time series at a spatial resolution of 0.05° (Funk et al., 2015). CHIRPS has been described as one of the most accurate datasets to represent the rainfall regime across Amazonia, demonstrating superior performance compared to other data sources when validated against station-based observations (Polasky et al., 2025; Silva et al., 2023). Validations across the basin have shown accuracy above 70% (Anderson et al., 2018; Mu et al., 2021; Paca et al., 2020). We resampled the CHIRPS dataset to match the 0.1° spatial resolution of the ERA5-Land dataset.

- Maximum cumulative water deficit (MCWD): We used CHIRPS to calculate the annual maximum cumulative water deficit (MCWD) from 1981 to 2024, an indicator of water stress in forests (Aragão et a., 2007). A water deficit occurs when evapotranspiration (ET) exceeds precipitation, with a 100 mm^{-month} ET threshold commonly applied for tropical forests (Aragão et a., 2007). However, increases in temperature have affected Amazonia's ET by increasing atmospheric evaporative demand (Malhi et al, 2009). To incorporate this warming effect, we calculated MCWD using fixed 100 mm^{-month} ET ($MCWD_{100}$) and temperature-linked ET ($MCWD_{temp}$). In this case, we considered that for each 1ºC above the mean temperature of a reference period (1971-1980), the 100 mm^{-month} ET threshold is increased by 8.9 mm $month^{-1}$. This coefficient is based on simple linear extrapolations of simulations of climatic scenarios that predict an increase of evapotranspiration in the Amazon forest to 140 mm^{-month} under conditions of increased temperature (4.7ºC) and CO_2 (850 ppm) (Malhi et al, 2009). Rescaling this adds 8.9 mm^{-month} for every 1 ºC increase in temperature, assuming atmospheric CO_2 concentrations and temperature increase linearly as per the model. We calculated the MCWD for both the fixed-ET ($MCWD_{100}$) and temperature-linked ET ($MCWD_{temp}$) using the R routine developed by Silva-Junior & Campanharo, (2021).

2. Determining the hydrological year

To assess trends in the climate variables, we defined a cell-wise hydrological year that follows Amazonia's highly variable precipitation cycle (e.g. Carvalho et al., 2021a) rather than a fixed (January-December) calendar year or predetermined months. This approach considers the pronounced spatiotemporal variation in the timing and length of wet/dry periods across the Amazonia. First, we aggregated the daily CHIRPS precipitation into 5-day periods (pentad), resulting in 73 pentads for each calendar year from 1981 to 2024. Leap days were removed from the analyses. Then, for each cell we calculated the annual mean precipitation of each pentad over the 44-year period and identified the pentad with the highest mean precipitation. For each cell, the pentads of the calendar year were reordered according to the position of the wettest peak pentad, becoming the first of the 73 pentads of each hydrological year. For example, if the wettest pentad occurs in the position 32 in the calendar year, the hydrological years for that cell span from pentad 32 of the current year (t) to pentad 31 of the next year (*t + 1)*, (Extended Data Figure S2).

We aggregated the daily statistics for the minimum, maximum and mean temperature and mean VPD into mean 5-day periods (pentads) and reordered these variables according to the hydrological year. For MCWD, we applied the same methodology, but as this metric is calculated based on monthly thresholds for evapotranspiration, the hydrological years were defined based on the month with the highest precipitation. Because the wettest pentad/month generally did not occur in the first pentad/month of the calendar year, the hydrological year covered periods that extended across two calendar years in 99.84% of cells in the pentad approach and in 84.31% in the monthly approach, demonstrating the unsuitability of calendar years for these assessments. As a result, even though the CHIRPS and ERA5-Land dataset were available for 44 years (1981–2024), only 43 complete hydrological years were available for trend analysis (1981–2023).

3. Determining driest and wettest periods of the year

To consider the spatiotemporal variation of precipitation across Amazonia (Carvalho et al., 2021a), we used the CHIRPS hydrological year time series to identify the driest period for each cell. To identify the onset and end of the driest period, we applied the methodology proposed by Fu et al., (2013)comparing the mean precipitation of each pentad with the annual mean precipitation over the 43-year period. The onset corresponds to the first pentad in a sequence of at least six out of eight consecutive pentads with precipitation below the baseline. Conversely, the end of the driest period corresponds to the first pentad in a sequence of at least six out of eight with precipitation above the baseline, (Extended Data Figure S1). The wettest period was defined as all pentads outside the driest period.

4. Data analysis

4.1 Set of variables analysed

We calculated mean values for the entire hydrological year and for the driest period for temperature variables (minimum, mean and maximum) and for mean VPD. For MCWD, we calculated the values for the entire hydrological year. For precipitation, we obtained the annual sum and the sum for both driest and wettest periods. The precipitation in the wettest period was calculated as the difference between the precipitation in the hydrological year and the driest period. Finally, we calculated the precipitation amplitude, by doing the difference between precipitation in the wettest and driest periods within the hydrological year.

4.2 Central and extreme trend analyses

To analyse central and extreme trends in climatic variables over time, we used non-parametric Quantile Generalized Additive Models (qGAM). We chose this model because it allowed us to test and obtain coefficients for central and extreme trends through percentile (*i.e.*, quantile) models, while still accounting for the temporal dependence of the data (analysis over years). To keep the trend analysis linear, we did not include a smoothing parameter to the term "hydrological year" [Response ~ hydrological year (1981-2023)]. For each cell and each variable, we ran a qGAM for the 50^{th} (median – central) and 5^{th} and 95^{th} (extremes) percentiles and obtained the coefficients which can be interpreted as the rates of change of a given variable (change in the variable per year). We did that using the function '*qgam'* from R package '*qgam'* (Fasiolo et al., 2021) in the R software (R Core Team, 2025).

To pinpoint the areas with greatest divergence between extreme and central trends, we subtracted the values of the decadal rates of change in the 50^{th} percentile from the rates of change in the extreme (95^{th} percentile for temperature and VPD and 5^{th} percentile for $MCWD_{temp}$) for mean temperature in the hydrological year, maximum temperature and VPD in the driest period of the hydrological year and $MCWD_{Temp}$ of the hydrological year. We selected the top and bottom 10% values of the difference between central and extreme rates of change (*i.e.*, 10% values for where extreme trends were higher than central trends and vice-versa) to display the average curves for the regions with greatest divergence between extreme and central trends. For this, we built the trend curves (50^{th} and 5^{th} / 95^{th} percentiles) for all the 5,790 cells (10% of cells – 5,735 cells for MCWD) based on their intercepts and coefficients and calculated the median curve and IQR (25-75 – 50% of the data distribution). To identify overlaps between regions with the highest rates of change of different climate variables, we selected the top 10% values of decadal rates of change for mean and maximum temperature, VPD and $MCWD_{temp}$ of the extreme (95^{th} percentile for temperature and VPD and 5^{th} percentile for $MCWD_{temp}$) and central (50^{th} percentile) trends.

4.3 Associations of rates of change with climatic initial conditions and agricultural lands

To investigate if climate change is spatially associated with the average climatic conditions at the start of the time series, we ran 1,000 bootstrap analyses of Spearman correlation, using 100 samples (cells) each time. We used the bootstrap approach because i) we wanted to have a confidence interval for the coefficients of correlation, ii) there is high spatial autocorrelation in the data, and iii) using > 50,000 points would increase the chances of type I error. We first calculated the mean values for each climatic variable in the period between 1981 and 1990. Then, for each combination of a variable, a percentile (5^{th}, 50^{th} and 95^{th}), a period (year, Driest Period - DP and Wettest Period - WP) and a method (100 mm threshold and Temp-linked threshold for MCWD) we used the '*cor.test*' function in R software to bootstrap the Spearman correlation test and obtained the coefficient of correlation (*r*) between the rate of change and the mean value (1981–1990) of a given variable. We defined the confidence intervals as the distribution of 95% of the *r* coefficients (2.5^{th} – 97.5^{th} percentiles) obtained from the 1000 bootstraps. We defined non-significant correlations as the ones that the confidence intervals crossed zero.

To investigate if the rates of change of climatic variables are spatially associated with previously deforested areas, we followed the same procedure as described above, but using the proportion of agricultural land in each cell against the rates of change of each variable. To obtain the current proportion of agricultural land in each cell, we used the MapBiomas Amazonia Collection 6 land-use and land-cover map (MapBiomas, 2025). We first calculated the area of each cell that was possible to be converted to agricultural lands by excluding the area occupied by the classes "Water" and "Urban infrastructure". We then extracted the area occupied by the class "Farming and silviculture" which included "Pasture", "Agriculture", "Silviculture", "Oil Palm" and "Mosaic of uses". Finally, we calculated the proportion occupied by agricultural lands by dividing the area occupied by "Farming and silviculture" by the remaining area after excluding water and urban areas. We then ran the 1000 bootstrap Spearman correlation tests (rates of change against proportion of agricultural lands) for each combination of variable, period, method (in the case of MCWD) and percentile. Because MCWD is a negative variable, we inverted the values to facilitate the interpretation of its association with agricultural lands (*i.e.*, positive correlation would mean higher deficit in cells with higher proportion of agricultural lands).

References (Methods)

Anderson, L. O., Neto, G. R., Cunha, A. P., Fonseca, M. G., De Moura, Y. M., Dalagnol, R., Wagner, F. H., & De Aragão, L. E. O. E. C. (2018). Vulnerability of Amazonian forests to repeated droughts. *Philosophical Transactions of the Royal Society B: Biological Sciences*, *373*, 1–12. https://doi.org/10.1098/rstb.2017.0411

Burton, C., Rifai, S., & Malhi, Y. (2018). Inter-comparison and assessment of gridded climate products over tropical forests during the 2015/2016 El Niño. *Philosophical Transactions of the Royal Society B: Biological Sciences*, *373*(1760). https://doi.org/10.1098/rstb.2017.0406

Carvalho, N. S., Anderson, L. O., Nunes, C. A., Pessôa, A. C. M., Silva Junior, C. H. L., Reis, J. B. C., Shimabukuro, Y. E., Berenguer, E., Barlow, J., & Aragão, L. E. O. C. (2021). Spatio-Temporal variation in dry season determines the Amazonian fire calendar. *Environmental Research Letters*, *16*(12). https://doi.org/10.1088/1748-9326/ac3aa3

Duursma, R. A. (2015). Plantecophys - An R package for analysing and modelling leaf gas exchange data. *PLoS ONE*, *10*(11). https://doi.org/10.1371/journal.pone.0143346

Fasiolo, M., Wood, S. N., Zaffran, M., Nedellec, R., & Goude, Y. (2021). qgam: Bayesian Nonparametric Quantile Regression Modeling in R. *Journal of Statistical Software*, *100*(9). https://doi.org/10.18637/JSS.V100.I09

Fu, R., Yin, L., Li, W., Arias, P. A., Dickinson, R. E., Huang, L., Chakraborty, S., Fernandes, K., Liebmann, B., Fisher, R., & Myneni, R. B. (2013). Increased dry-season length over southern Amazonia in recent decades and its implication for future climate projection. *Proceedings of the National Academy of Sciences of the United States of America*, *110*(45), 18110–18115. https://doi.org/10.1073/pnas.1302584110

Funk, C., Peterson, P., Landsfeld, M., Pedreros, D., Verdin, J., Shukla, S., Husak, G., Rowland, J., Harrison, L., Hoell, A., & Michaelsen, J. (2015). The climate hazards infrared precipitation with stations - A new environmental record for monitoring extremes. *Scientific Data*, *2*. https://doi.org/10.1038/sdata.2015.66

MapBiomas. (2025). *MapBiomas Amazonian Project - Collection 6 of the Annual Land Use and Land Cover Maps of Amazonian, accessed on 12 January through the link: [https://amazonia.mapbiomas.org/en/mapbiomas-amazonia-collection/]*. https://mapbiomas.org/

Mu, Y., Biggs, T., & Shen, S. S. P. (2021). Satellite-based precipitation estimates using a dense rain gauge network over the Southwestern Brazilian Amazon: Implication for identifying trends in dry season rainfall. *Atmospheric Research*, *261*. https://doi.org/10.1016/j.atmosres.2021.105741

Muñoz-Sabater, J., Dutra, E., Agustí-Panareda, A., Albergel, C., Arduini, G., Balsamo, G., Boussetta, S., Choulga, M., Harrigan, S., Hersbach, H., Martens, B., Miralles, D. G., Piles, M., Rodríguez-Fernández, N. J., Zsoter, E., Buontempo, C., & Thépaut, J. N. (2021). ERA5-Land: A state-of-the-art global reanalysis dataset for land applications. *Earth System Science Data*, *13*(9), 4349–4383. https://doi.org/10.5194/essd-13-4349-2021

Paca, V. H. da M., Espinoza-Dávalos, G. E., Moreira, D. M., & Comair, G. (2020). Variability of trends in precipitation across the Amazon river basin determined from the CHIRPS precipitation product and from station records. *Water (Switzerland)*, *12*(5). https://doi.org/10.3390/W12051244

Polasky, A., Sapkota, V., Forest, C. E., & Fuentes, J. D. (2025). Discrepancies in precipitation trends between observational and reanalysis datasets in the Amazon Basin. *Scientific Reports*, *15*(1). https://doi.org/10.1038/s41598-025-87418-5

R Core Team. (2025). *R: A Language and Environment for Statistical Computing*. https://cran.r-project.org/faqs.html

RAISG, A. N. of G. S.-E. I. (2024). *RAISG 2024*. https://www.raisg.org/en/about/

Sarkar, S., & Maity, R. (2021). Global climate shift in 1970s causes a significant worldwide increase in precipitation extremes. *Scientific Reports*, *11*(1). https://doi.org/10.1038/s41598-021-90854-8

Silva, F. D. dos S., da Costa, C. P. W., dos Santos Franco, V., Gomes, H. B., da Silva, M. C. L., dos Santos Vanderlei, M. H. G., Costa, R. L., da Rocha Júnior, R. L., Cabral Júnior, J. B., dos Reis, J. S., Cavalcante, R. B. L., Tedeschi, R. G., de Jesus da Costa Barreto, N., Nogueira Neto, A. V., dos Santos Jesus, E., & da Silva Ferreira, D. B. (2023). Intercomparison of Different Sources of Precipitation Data in the Brazilian Legal Amazon. *Climate*, *11*(12). https://doi.org/10.3390/cli11120241

Silva-Junior, C. H. L., & Campanharo, W. A. (2021). *Maximum Cumulative Water Deficit - MCWD: a R language script (v1.1.0) (v1.1.0). Zenodo.* https://doi.org/https://doi.org/10.5281/zenodo.5034650

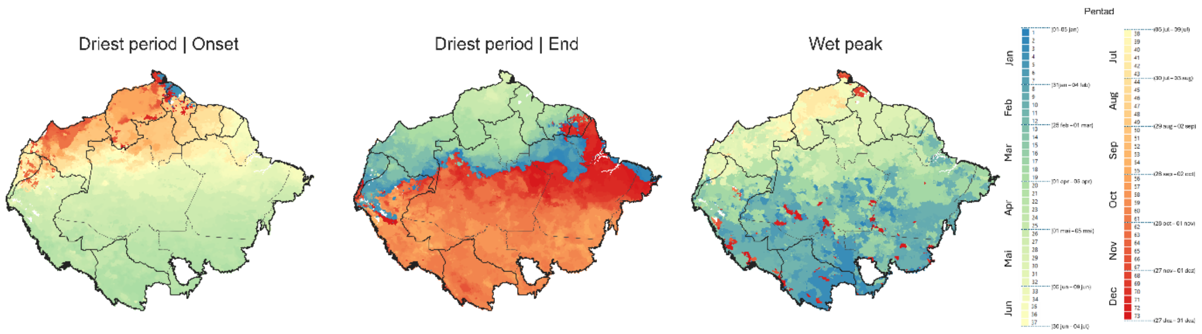

Extended Data Figure S1. Spatiotemporal patterns of the driest and wettest period of the calendar year. Onset of the driest period is defined by the first pentad in a sequence of at least six out of eight consecutive pentads with precipitation below the baseline; the end of the driest period is defined analogously. Pentad 1 corresponds to 1–5 January and pentad 73 to 27–31 December. The wet peak corresponds to the pentad with the highest mean precipitation in the historical period (1981 – 2024) and is the reference for converting the calendar year to hydrological year.

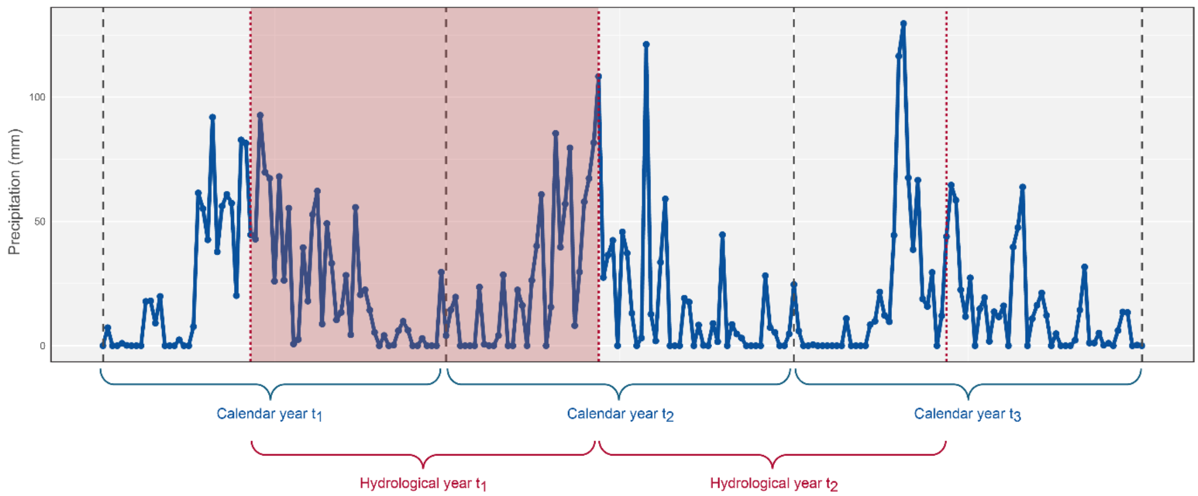

Extended Data Figure S2. Definition of the hydrological year. Calendar year is divided into 73 pentads (5-day periods), from 1–5 January (pentad 1) through 27–31 December (pentad 73). The hydrological year is defined as a contiguous sequence of 73 pentads beginning in the pentad with the highest mean precipitation based on the historical period (1981 – 2024). The first pentad of the hydrological year is the wettest pentad, which will be variable for each cell.

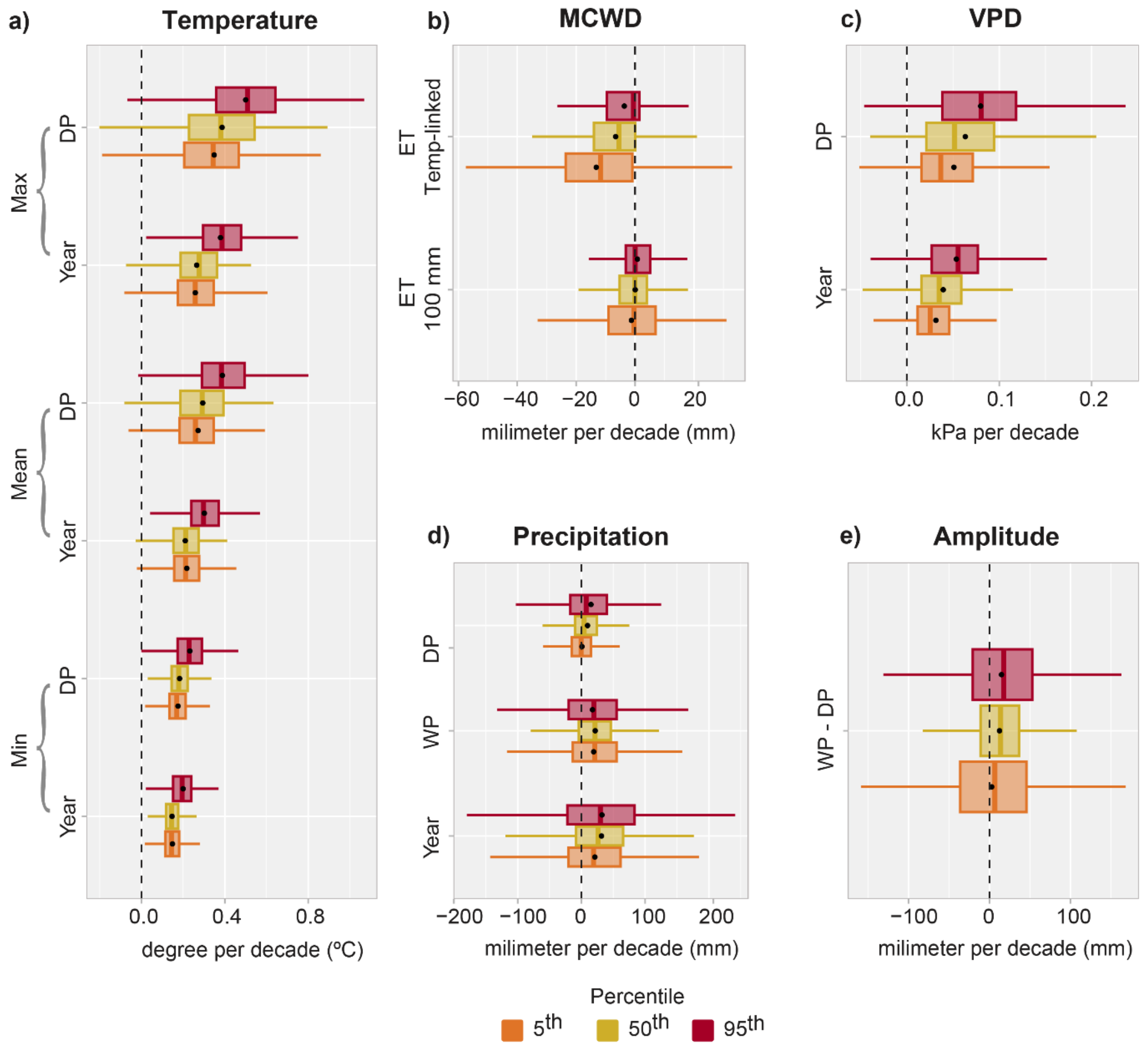

Extended Data Figure S3. The magnitude of climate change across the Amazon. Decadal rates of change of **a,** temperature (ºC dec^{-1}) **b,** maximum cumulative water deficit (MCWD, mm dec^{-1}) **c,** vapour-pressure deficit (VPD; kPa dec^{-1}), **d,** precipitation (mm dec^{-1}) and **e,** precipitation amplitude (mm dec^{-1}). All panels show the central (50th percentile) and extreme (5th and 95th percentiles) rate of change for the Amazon region calculated on grid cell-wise with a spatial resolution of 11 km. Trends for minimum, mean and maximum temperature and mean VPD were calculated for the hydrological year (Year) and driest period (DP). MCWD was calculated considering two evapotranspiration (ET) thresholds, one fixed at 100 mm and the other linked to temperature. Precipitation trends included the hydrological year, DP and the wettest period (WP). Precipitation amplitude is the difference between rainfall in the wettest and driest period. In all panels, black dots represent the Amazon-wide mean rate of change per decade of each variable in each percentile in each period. Dashed vertical lines corresponds to zero. Outliers are not shown to restrict axes to the main trends.

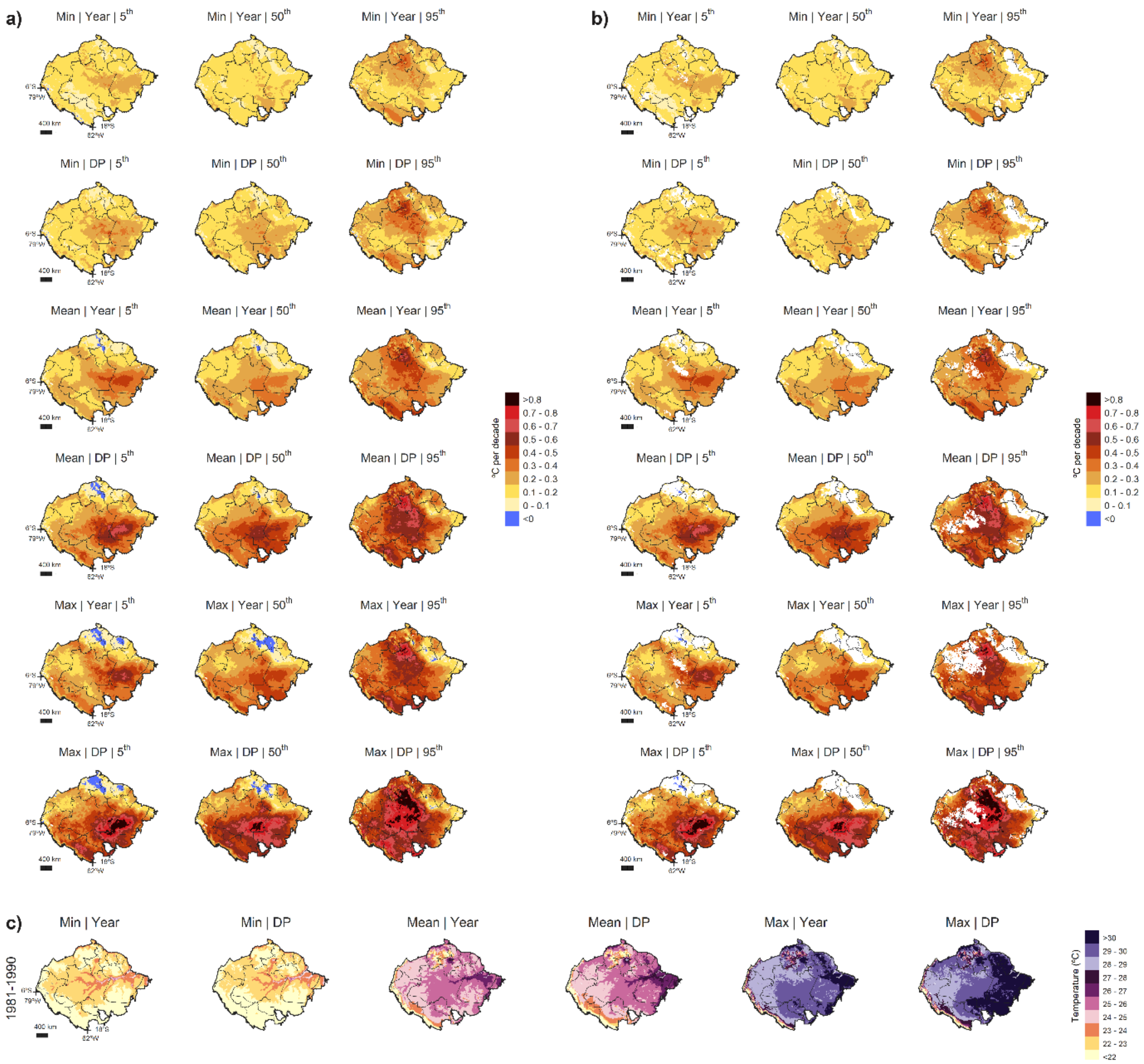

Extended Data Figure S4. Spatial distribution of temperature change across the Amazon. a, Basin wide and **b,** statistically significant (p<0.05 decadal rates of change (ºC dec^{-1}) for minimum (Min), mean and maximum (Max) temperature. In the rate of change, central trend (50th percentile) and extremes quantiles (5th and 95th percentiles) are shown for the hydrological year (Year) and driest period (DP). In panel b, non-significant values are indicated in white. **c,** historical average values for the reference period (1981-1990) for the minimum, mean and maximum temperature during the hydrological year and driest period.

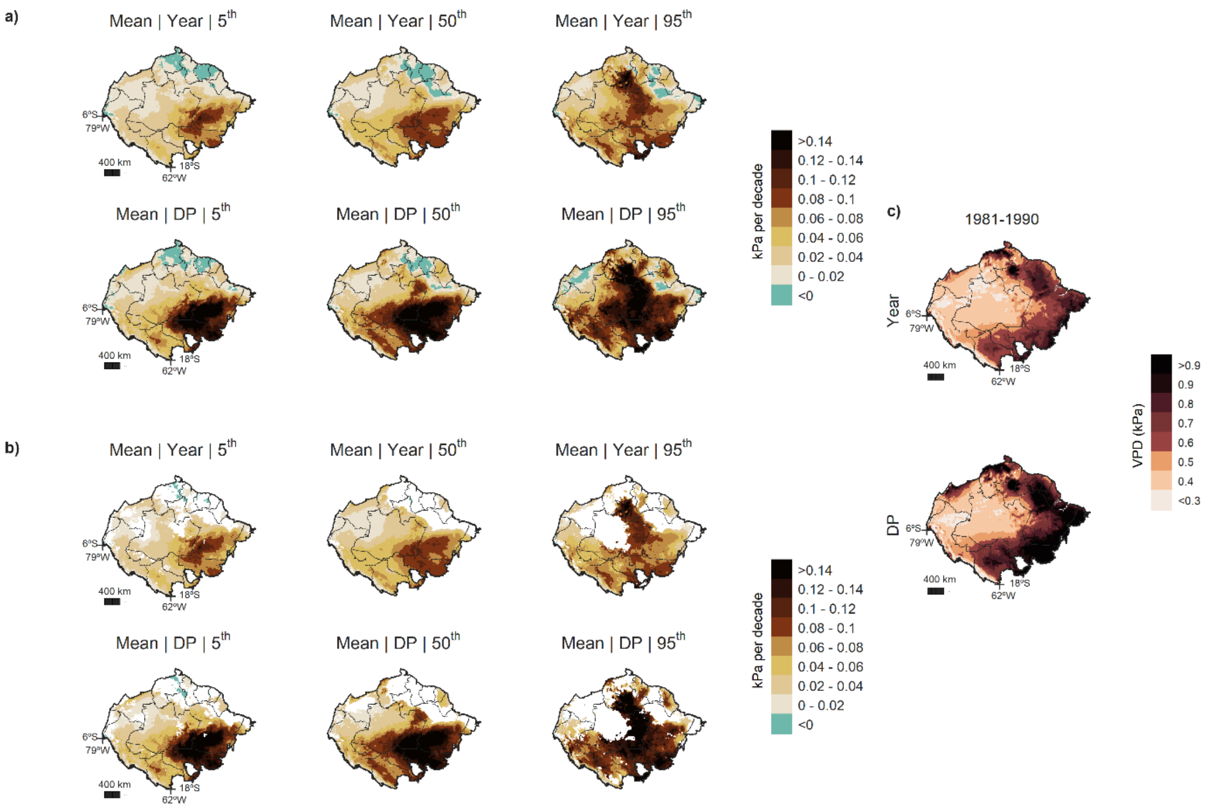

Extended Data Figure S5. Spatial distribution of vapour-pressure deficit (VPD) change across the Amazon. a, Basin wide and **b,** statistically significant ($p<0.05$) decadal rates of change (kPa dec^{-1}) for mean VPD. In the rate of change, central trend (50th percentile) and extremes quantiles (5th and 95th percentiles) are shown for the hydrological year (Year) and driest period (DP In panel b, non-significant values are indicated in white. **c,** historical average for the reference period (1981-1990) for the mean VPD during the hydrological year and driest period.

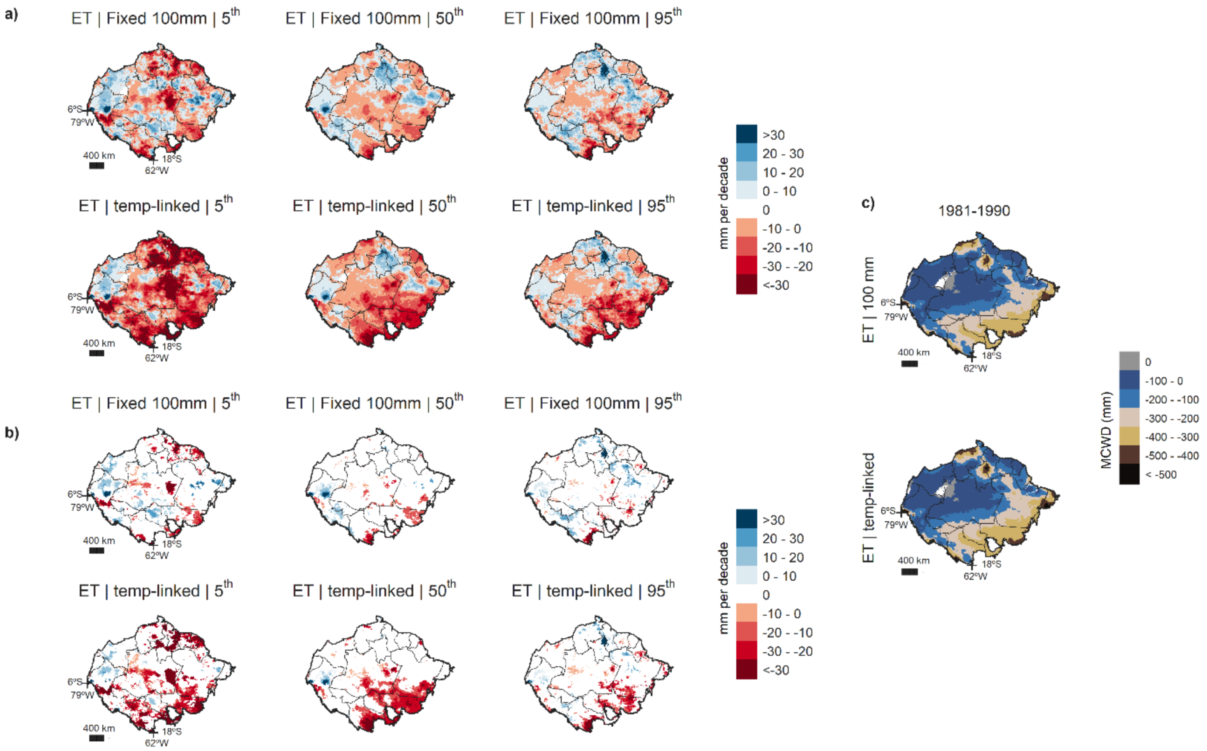

Extended Data Figure S6. Spatial distribution of maximum cumulative water deficit (MCWD) change across the Amazon. a, Basin wide and **b,** statistically significant ($p<0.05$) decadal rates of change (mm dec^{-1}) for MCWD for central trend (50th percentile) and extremes quantiles (5th and 95th percentiles) considering a fixed evapotranspiration (ET) of 100 mm and for the 5% quantile with a temperature-linked ET. In panel b, non-significant values are indicated in white. **c,** historical average for MCWD for with fixed and temperature-linked ET for the reference period (1981-1990).

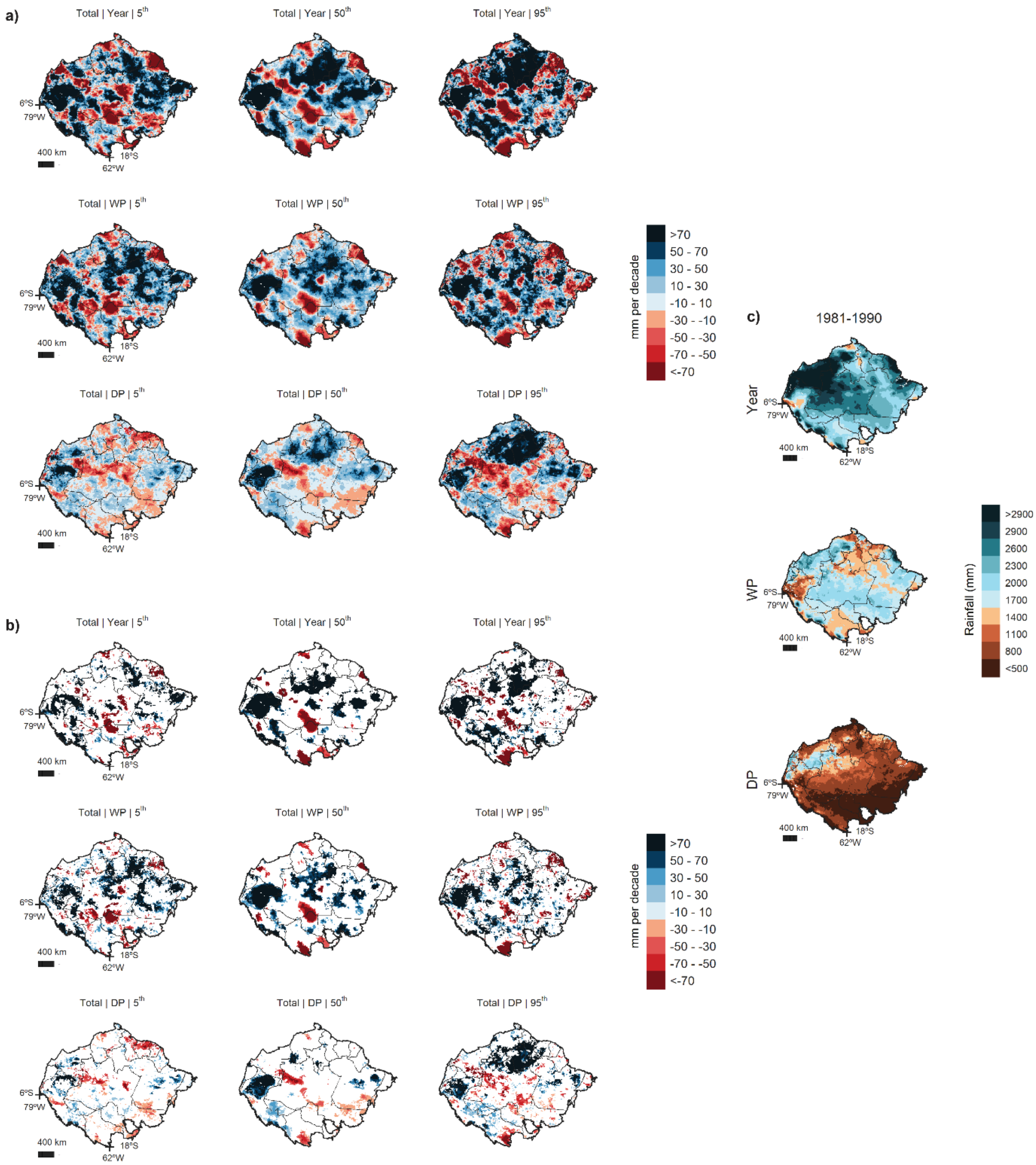

Extended Data Figure S7. Spatial distribution of precipitation change across the Amazon. a, Basin wide and **b,** statistically significant (p<0.05 decadal rate of change (mm dec^{-1}) for precipitation. In the rate of change, central trend (50th percentile) and extremes quantiles (5th and 95th percentiles) are shown for the hydrological year (Year), driest (DP) and wettest period (WP). In panel b, non-significant values are indicated in white. **c,** historical average values for the reference period (1981-1990) for the precipitation during the hydrological year, WP and DP.

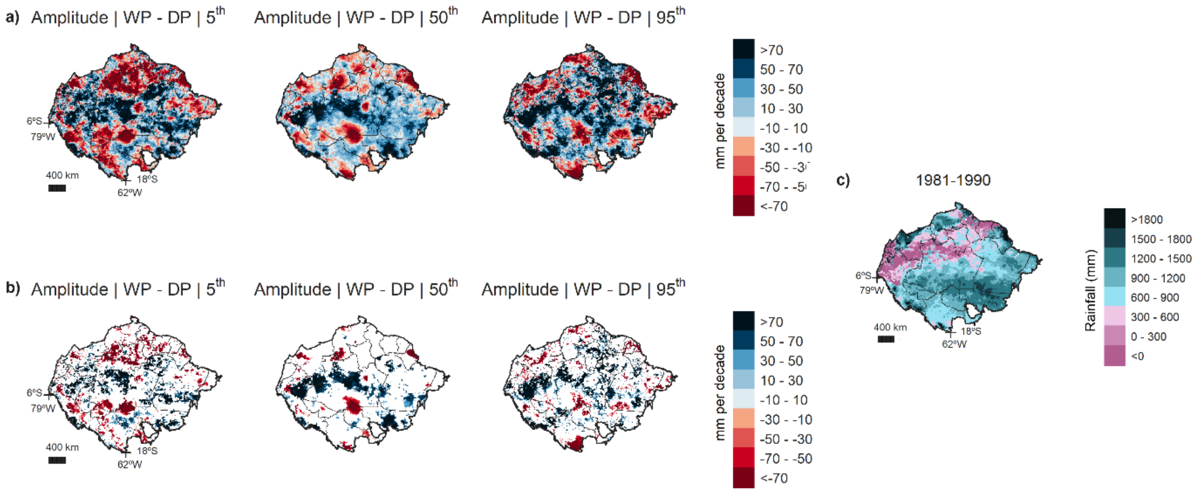

Extended Data Figure S8. Spatial distribution of amplitude precipitation change across the Amazon. a, Basin wide and **b,** statistically significant ($p<0.05$) decadal rates of change (mm dec^{-1}) for amplitude of precipitation for the central trend (50^{th} percentile) and extremes quantiles (5^{th} and 95^{th} percentiles) during the hydrological year. Amplitude of precipitation is the difference between the rate of change in the wettest and driest period. Non-significant values are indicated in white in panel (b). **c,** historical average of amplitude precipitation for the reference period (1981-1990).

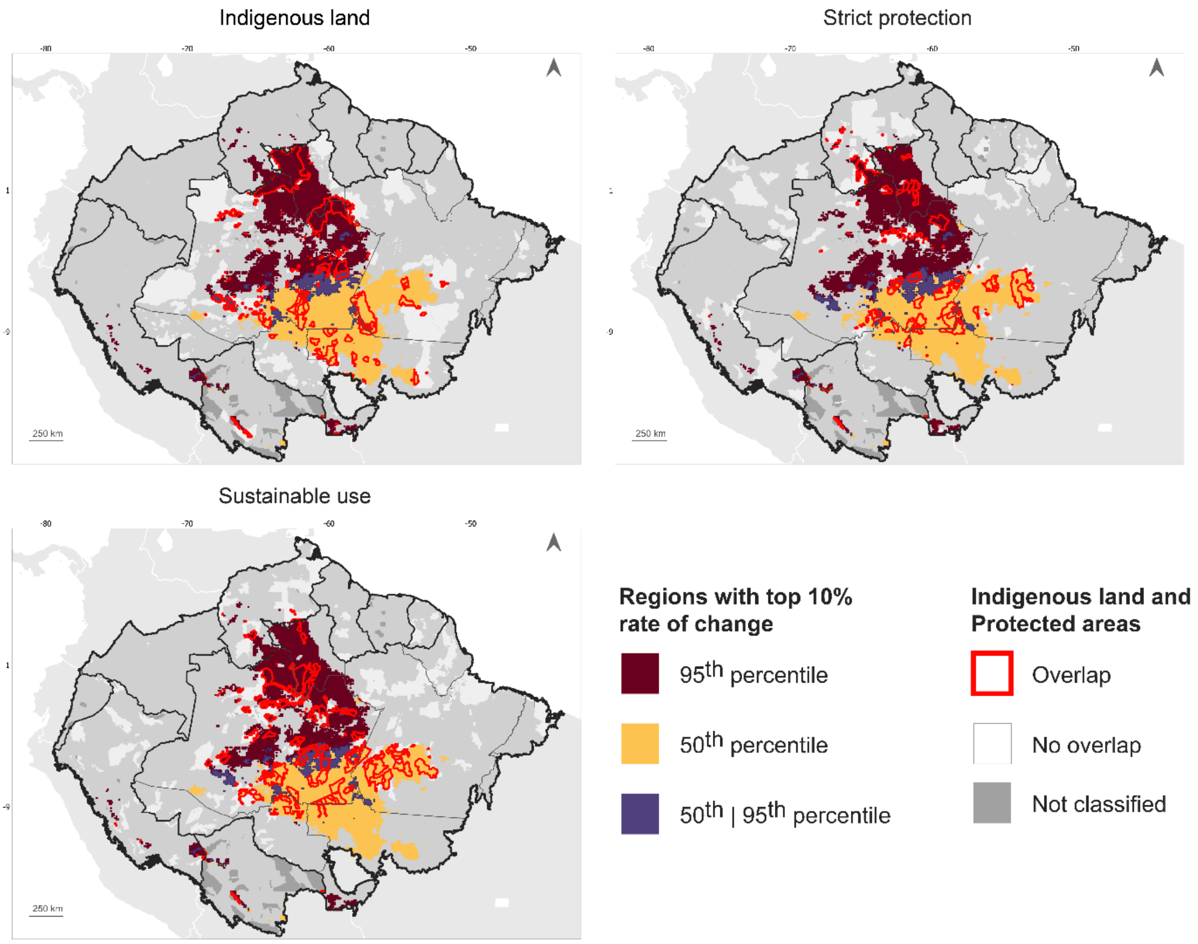

Extended Data Figure S9. Protected areas affected by the highest increase in temperature in the Amazon. The regions with the top 10% rate of increase in maximum temperature in the driest period are shown in yellow for the central trend (50^{th}

percentile), dark red for the extreme (95th percentile), and purple where the two overlap. The protected areas were obtained from the World Database on Protected Area (WDPA). We reclassified the all the protected areas within the Amazon region into Indigenous Land, Strict Protection and Sustainable Use. All protected areas that had an indication of being an indigenous land in the title were reclassified as Indigenous Land. We reclassified the remaining protected areas as Strict protection when they were originally within the groups Ia, Ib, II, III and IV and as Sustainable use when they were originally within the groups V and VI of IUCN classification. All indigenous lands, and strict protection and sustainable use protected areas are shown in white and when they overlap the regions with highest increase in temperature, they have the borders of the overlap in red. The protected areas indicated as "Not reported", "Not Assigned", "Not Applicable" in WDPA were reclassified to "Not classified" and are shown in dark grey.

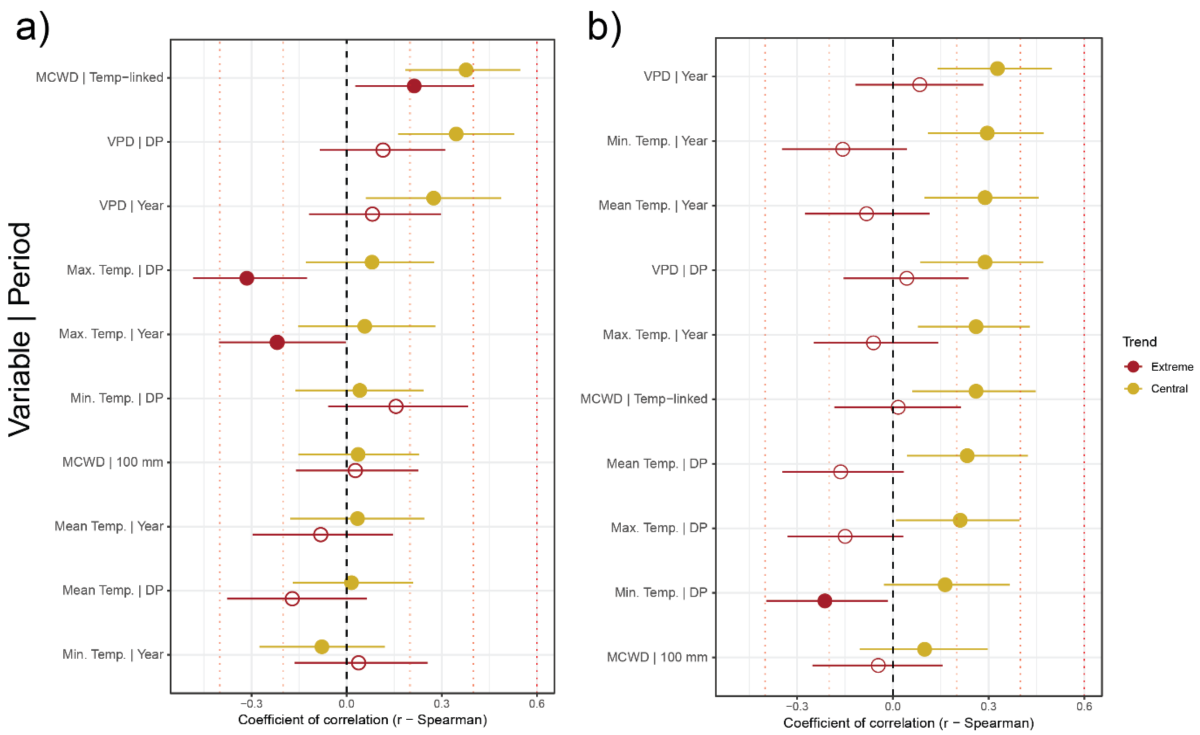

Extended Data Figure S10. Spatial associations between climate change, climate means and agricultural land cover. Amazon-wide correlations between the decadal rates of change of climatic variables and **a,** their mean values (1981-1990) and **b,** the proportion of agricultural lands in each 11km cell. For each combination of a variable, a percentile (50th and 95th), a period (Year, Driest Period – DP) and a method (100 mm threshold and Temp-linked threshold for MCWD) we ran 1000 bootstrap analysis of Spearman correlation, using 100 samples to build a confidence interval for the associations. Non-significant associations are represented by hollow symbols. Variables were ordered by mean correlation coefficients in the central (50th) trend. Red dashed lines are drawn at r = +-0.2, +-0.4 and 0.6. Temp = Temperature, VPD = vapour-pressure deficit, MCWD = maximum cumulative water deficit.